

Subtropical to Subpolar Lagrangian Pathways in the North Atlantic and Their Impact on
High Latitude Property Fields

by

Kristin Cashman Burkholder

Department of Earth and Ocean Sciences
Duke University

Date: _____ July 28, 2011 _____

Approved:

Susan Lozier, Supervisor

Paul Baker

Peter Haff

John Bane

Dissertation submitted in partial fulfillment of
the requirements for the degree of
Doctor of Philosophy in the Department of
Earth and Ocean Sciences in the Graduate School
of Duke University

2011

ABSTRACT

Subtropical to Subpolar Lagrangian Pathways in the North Atlantic and their Impacts on

High Latitude Property Fields

by

Kristin Cashman Burkholder

Department of Earth and Ocean Sciences
Duke University

Date: _____ July 28, 2011 _____

Approved:

Susan Lozier, Supervisor

Paul Baker

Peter Haff

John Bane

An abstract of a dissertation submitted in partial fulfillment of the requirements for the degree of Doctor of Philosophy in the Department of Earth and Ocean Sciences in the Graduate School of Duke University

2011

Copyright by
Kristin Cashman Burkholder
2011

Abstract

In response to the differential heating of the Earth, the atmosphere and ocean advect surplus energy from low to high latitudes. In the ocean, this poleward energy flux occurs as part of the large scale meridional overturning circulation: warm, shallow waters are transported to high latitudes where they cool, sink and then follow subsurface pathways equatorward until they are once again upwelled to the surface and reheated. In the North Atlantic, the upper limb of this circulation has traditionally been associated with the Gulf Stream/North Atlantic Current system that carries warm surface waters to the subpolar region. This advection is believed to be responsible for the elevated sea surface temperatures in the eastern subpolar gyre, which, because the prevailing winds sweeping across the Atlantic are warmed by these waters, produce anomalously warm temperatures in Western Europe. This view has long been supported by Eulerian measurements of North Atlantic sea surface temperature and surface velocities, which imply a direct and continuous transport of surface waters between the two gyres. However, though the importance of this redistribution of heat from low to high latitudes has been broadly recognized, few studies have focused on this transport within the Lagrangian frame.

The three studies included in this dissertation use data from the observational record and from a high resolution model of ocean circulation to re-examine our understanding of upper limb transport between the subtropical and subpolar gyres. Specifically, each chapter explores intergyre Lagrangian pathways and investigates the impact of those

pathways on subpolar property fields. The findings from the studies suggest that intergyre transport pathways are primarily located beneath the surface and that subtropical surface waters are largely absent from the intergyre exchange process. Additionally, these studies highlight the importance of examining transport pathways using 3d velocity fields.

Contents

Abstract	iv
List of Tables	viii
List of Figures	ix
1. Introduction.....	1
2. Subtropical to Subpolar Lagrangian Pathways in the Eastern North Atlantic and Their Impacts on High Latitude Salinity Fields	4
2.1 Introduction.....	4
2.2 Background.....	8
2.3 Data and Methods	10
2.3.1 Observational Data.....	11
2.3.2 FLAME Data	12
2.4 Results and Discussion	16
2.4.1 What are the pathways that carry MOW to the eastern subpolar gyre?.....	16
2.4.2 Changing High Latitude Salinities and the Circulation of the Subpolar Gyre.	20
2.4.3 Lagrangian Pathways to the Rockall Trough.....	24
2.5 Summary	33
3. Subtropical to Subpolar Pathways in the North Atlantic: Deductions from Lagrangian Trajectories	35
3.1 Introduction.....	35
3.2 Background.....	36
3.3 Methods.....	41
3.4 Results.....	45

3.4.1 Can surface drifters from the observational record provide an accurate assessment of surface intergyre exchange and its temporal variability?	45
3.4.1.1 What are the effects of variable launch locations and the constraint of drifter movement to a 2d surface on the measure of intergyre exchange?	48
3.4.1.2 Could the removal of Ekman velocities allow for a meaningful measure of exchange by surface drifters?.....	53
3.4.2 Is the amount of intergyre exchange at the surface representative of the overall subtropical to subpolar exchange?	57
3.5 Summary	67
4. Understanding the Oceanic Transport of Heat to the Eastern Subpolar Gyre	69
4.1 Introduction and Background	69
4.2 Methods.....	73
4.3 Results.....	75
4.3.1 Determination of Lagrangian Pathways Supplying the ESG.....	75
4.3.1.1 The Subpolar Pathway	77
4.3.1.2 The Subtropical Pathway	84
4.3.2 Connection to <i>Burkholder and Lozier (2011)</i>	91
4.4 Summary	93
References.....	96
Biography.....	101

List of Tables

Table 1: Percent of RAFOS and synthetic floats reaching the Rockall Trough and subpolar gyre with lifetimes of 2 and 5 years	18
Table 2: Percent of drifters drogued to 15 m that reach 53°N when launched from various launch locations and advected through various horizontal velocity fields	51
Table 3: Percent of floats launched at 15 m that reach 53°N when launched from various launch locations and advected in 3d through various velocity fields.	53
Table 4: Number of floats launched at various depths within the eastern subpolar gyre that reached the eastern subpolar gyre via the subtropical and subpolar pathways.....	77
Table 5: Mean depth of floats launched at various depths within the eastern subpolar gyre when they cross the 32°N or 60°N boundary	84
Table 6: Mean change in temperature of floats as they progress along the subtropical and subpolar pathways to the eastern subpolar gyre	85

List of Figures

Figure 1: Diagnostic velocity field superposed on the mean salinity field along the $\sigma_{0.5}=29.90$ density surface [from <i>Iorga and Lozier, 1999b</i>]	5
Figure 2: Trajectories of RAFOS floats released between 1996 and 1997 and grouped according to launch position	7
Figure 3: Isopycnal contours at the entry of the Rockall Trough shown over the mean subtracted salinity anomalies	14
Figure 4: Trajectories of 23 synthetic floats launched in FLAME in December, 1996 from the locations of the RAFOS floats	19
Figure 5: Average zonal shift in the position of the subpolar front at 55°N in FLAME compared with the smoothed Häkkinen and Rhines gyre index	22
Figure 6: Salinity fields in high and low gyre index years along the MOWmod isopycnal in FLAME	23
Figure 7: Mean subtracted anomalies in the Rockall Trough along the MOWmod isopycnal in FLAME and the MOWobs isopycnal in the observational record	25
Figure 8: Trajectories of 100 randomly selected floats released from the Rockall Reverse launch positions and run backwards in time for 6 years	26
Figure 9: Number of floats released from the Rockall Trough launch line which passed through the MAR and ENA launch lines	30
Figure 10: Percent of floats arriving in the Rockall Trough through the MAR and ENA lines	32
Figure 11: Mean velocities, temperatures and transports in FLAME	37
Figure 12: Comparison of EKE fields from surface drifters and satellite measurements with the EKE field from FLAME	43
Figure 13: Launch location schemes	46
Figure 14: Four year synthetic trajectories at 15 m for three modeled pentads	49
Figure 15: Effect of drifter lifetime on the delivery of 50 m drifters, beneath the Ekman layer, to the subpolar domain	56

Figure 16: Relationship between launch positions and pentad of the modeled circulation in the delivery of 50 m drifters to the subpolar domain.....	58
Figure 17: Statistics for Lagrangian floats which reach 53°N.....	60
Figure 18: Changes in velocities and synthetic float trajectories with depth in FLAME..	62
Figure 19: Isopycnal structure along 40°W in FLAME	64
Figure 20: Potential vorticity fields in FLAME.....	66
Figure 21: Climatologically averaged temperatures at 50 m in FLAME	72
Figure 22: Trajectories of floats advected backwards in time from the ESG.....	76
Figure 23: Population density plots for floats arriving at 60°N.....	79
Figure 24: Depths of 50 randomly selected floats run backwards in time to their origin in the western subpolar gyre	80
Figure 25: Temperature anomalies of 50 randomly selected floats run backwards in time to their origin in the western subpolar gyre..	81
Figure 26: Salinity anomalies of 50 randomly selected floats run backwards in time to their origin in the western subpolar gyre..	82
Figure 27: Density anomalies of 50 randomly selected floats run backwards in time to their origin in the western subpolar gyre.	83
Figure 28: Population density plots for floats arriving at 32°N.....	86
Figure 29: Temperature anomalies of 50 randomly selected floats run backwards in time to their origin in the western subtropical gyre	87
Figure 30: Salinity anomalies of 50 randomly selected floats run backwards in time to their origin in the western subtropical gyre	88
Figure 31: Depths of 50 randomly selected floats run backwards in time to their origin in the western subtropical gyre.	89
Figure 32: Density anomalies of 50 randomly selected floats run backwards in time to their origin in the western subtropical gyre.	90
Figure 33: Re-creation of Figure 17 in density space	94
Figure 34: Population density plot for floats arriving at 63°W.	95

Acknowledgements

I have been lucky that during my time in graduate school, I have been surrounded by a fantastic network of colleagues, family and friends who have provided a wonderful support system while I pursued my degree. A few members deserve specific acknowledgement and gratitude for their roles, especially:

Susan Lozier- who told me from the very beginning that graduate school is more about the journey than about the specifics of a thesis. She pushed me to remove my blinders and to think critically and deeply about topics great and small. I admire her for many things, including her amazing ability to multitask, her unwavering support of all of her graduate students, and her dedication to both her work and her family. It has been my honor to work as one of her students.

John Bane, Peter Haff and Paul Baker- for their support as members of my Ph.D. committee. All three were active and engaging participants, and provided valuable feedback as my thesis took shape. I appreciated their dedication, both to my education and to me as a student.

Christine Hebling and Chris Wilson- both of whom went before me down the Ph.D. road and offered friendship, inspiration, guidance and encouragement whenever I waivered. I adore them both.

Meg Newell- for her friendship and support, as well as her willingness to let me stay at her house every week for 3 years. I'm really going to miss our weekly check-ins and will forever be grateful to her for helping me make my life work for the past few years.

Stefan Gary and Apurva Dave- who make up 2/3 of the "triplets." They have been wonderful colleagues and friends since the day the three of us arrived on campus in 2006. We've gone through all the ups and downs of graduate school together, while sharing the happiness and trials of our lives for 5 years. Of all the wonderful people I've met at Duke, I'll miss them the most.

Mom, Dad, Meg and Kaela Cashman and Kate Smethurst- the people who have always cheered the longest and loudest for me no matter what I take on. Without knowing a thing about my program, they never once doubted that I could handle all the challenges that it presented. I appreciate their unwavering support, their encouragement and their willingness to handle stressed out phone calls. I love them all!

And most of all, to my husband **Andrew Burkholder**- who reminds me every day why I married him. I am so grateful to him for all the big and little things that he has done to lighten my load and to make me laugh, not just throughout my time in graduate school but in all of our years together. I love and appreciate him more than I could ever say.

1. Introduction

Traditionally, oceanographers have described the meridional overturning circulation in the following manner: warm surface waters are transported to high latitudes where they cool and sink, then follow subsurface pathways equatorward until they upwell to the surface and return to high latitudes. The upper limb of this circulation has been thought to be dominated by the transport of warm surface waters via the Gulf Stream and North Atlantic Current in a continuous path between the North Atlantic subtropical and subpolar gyres. This poleward transport of heat has been linked to the warm sea surface temperatures of the eastern subpolar gyre and in turn, the moderate temperatures of Western Europe. However, though the importance of the low to high latitude transport of warm waters has been broadly recognized, the nature of the Lagrangian transport between the subtropical and subpolar gyres has remained poorly understood. As such, this dissertation investigates the nature of the poleward flow by identifying and characterizing various subtropical to subpolar Lagrangian pathways and examining their impact on high latitude property fields.

The first study included in this work investigates the role of Mediterranean Overflow Water (MOW) in creating subsurface salinity anomalies within the Rockall Trough, a gateway to high latitude areas of deep convection in the Norwegian-Greenland Sea. Utilizing Lagrangian trajectories compiled from both synthetic and observational datasets, this study identifies two main density neutral transport pathways that supply the

Rockall Trough. One pathway, stretching along the path of the North Atlantic Current, involves the transport of relatively fresh waters to the eastern North Atlantic; the other transports salty waters northward from the MOW reservoir in the eastern subtropical gyre. The study findings indicate that changes in the relative contributions of these two pathways over time result in the observed mid-depth salinity anomalies in the Rockall Trough.

The second major component of this work examines the transport of synthetic drifters from the northwestern subtropical gyre to the subpolar gyre of the North Atlantic when launched from a variety of thermocline depths. The results of this study indicate that subtropical to subpolar exchange primarily occurs along subsurface pathways: though less than 5% of floats launched at 15 m reach the subpolar gyre within 4 years, while close to 30% of drifters launched at 700 m do so. As such, this study also points to the inability of drifters in the observational record, restricted to movement along the 15 m depth surface, to reconstruct Lagrangian pathways between the subtropical and subpolar gyres.

Finally, the third study in this work investigates the Lagrangian pathways that lead to the region of elevated sea surface temperatures in the eastern subpolar gyre and the impact of those pathways on the property fields in that region. Though evidence from the observational dataset has suggested that the major source of surface waters to the eastern subpolar gyre is recirculated surface waters from the western subpolar gyre, the findings

from this study indicate that the surface pathway connecting the western and eastern subpolar gyre plays only a small role in supplying the eastern surface waters. Instead, the findings suggest that the subsurface pathway following the path of the Gulf Stream, identified in the previous study, is the dominant pathway leading to the region and the largest oceanic source of heat to the surface waters.

2. Subtropical to Subpolar Lagrangian Pathways in the Eastern North Atlantic and Their Impacts on High Latitude Salinity Fields

2.1 Introduction

Observational evidence spanning 60 years indicates that the Rockall Trough, an entryway for North Atlantic waters to enter high latitude regions of deep convection [Ellet *et al.*, 1986; Holliday *et al.*, 2000], has experienced strong interannual and decadal scale variability in salinity and temperature at intermediate depths since the 1950s [Holliday *et al.*, 2000; Holliday, 2003; Lozier and Stewart, 2008]. Today, it is largely understood that this variability primarily results from wind-driven changes to the regional circulation patterns of the northeastern North Atlantic: when the winds over the subpolar gyre weaken (strengthen), the position of the eastern limb of the subpolar gyre shifts offshore (shoreward) resulting in an increased (decreased) contribution of warm and salty waters from the eastern North Atlantic to the Rockall Trough inflow [Holliday, 2003; Hátún *et al.*, 2005; Lozier and Stewart, 2008]. Interestingly, the subsurface salinity anomalies (relative to a climatological mean) in the Trough are situated at ~1100 m, suggesting the presence of Mediterranean Overflow Water (MOW), a warm and salty water mass principally residing at mid-depths in the eastern subtropical North Atlantic [Reid, 1979; Iorga and Lozier, 1999a; Iorga and Lozier, 1999b]. Indeed, mid-depth property changes within the Rockall Trough [Lozier and Stewart, 2008] and at latitudes as far north as

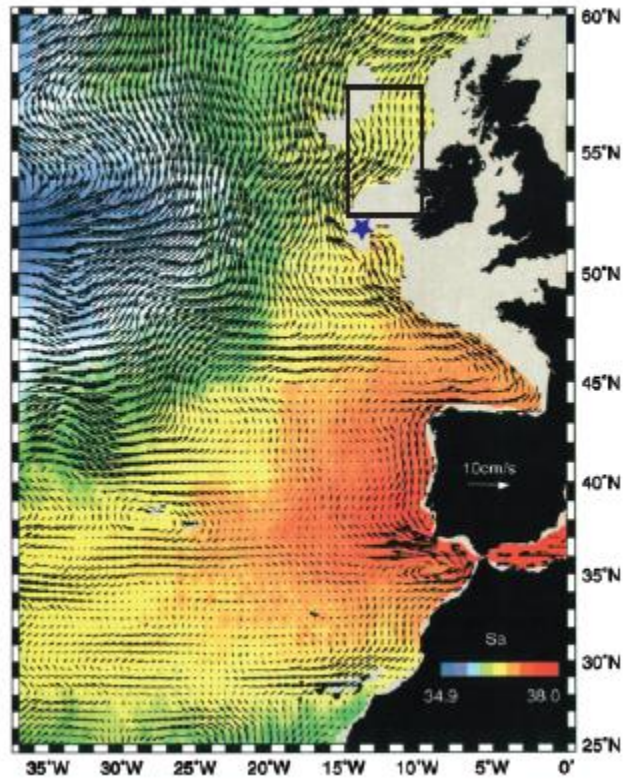


Figure 1: Diagnostic velocity field superposed on the mean (1909-1990) salinity field along the $\sigma_{0.5} = 29.90$ density surface [from *Iorga and Lozier, 1999b*]. The $\sigma_{0.5} = 29.90$ density surface was chosen by Iorga and Lozier to be representative of the MOW. Black box indicates the position of the Rockall Trough box used for analysis of salinity anomalies in this study. Blue star marks the position of Porcupine Bank.

60°N [*Sarafanov et al.*, 2008] have been linked to the intermittent influence of MOW. However, despite this implication, little is known to date about the actual mean and time-varying pathways by which MOW reaches those regions.

While mean salinity and diagnostic velocity fields at the depth of the MOW reservoir suggest that MOW may be transported to high latitudes by a continuous mid-depth current that extends northward along the eastern North Atlantic and into the Rockall Trough [Figure 1; *Reid*, 1979; *Iorga and Lozier*, 1999a; *Iorga and Lozier*, 1999b], the pathways of RAFOS floats launched between 1996 and 1997 at the depth of the MOW along the eastern boundary of the North Atlantic [Figure 2a-d; *Furey et al.*, 2001] reveal far more temporal and spatial variability for the northward penetration of MOW than that suggested by the Eulerian mean fields. As such, two questions are raised: (1) What are the pathways that carry MOW to the eastern subpolar gyre and specifically, to the Rockall Trough and (2) Can variability in MOW pathways explain the observed salinity anomalies in this region? To address these questions, pathways of RAFOS floats launched in the eastern North Atlantic, as well as pathways of synthetic floats launched in an ocean general circulation model (OGCM), are analyzed. Background for this study is contained in Section 2.2, data and methods are discussed in Section 2.3, followed by a discussion of study results in Section 2.4 and a summary in Section 2.5.

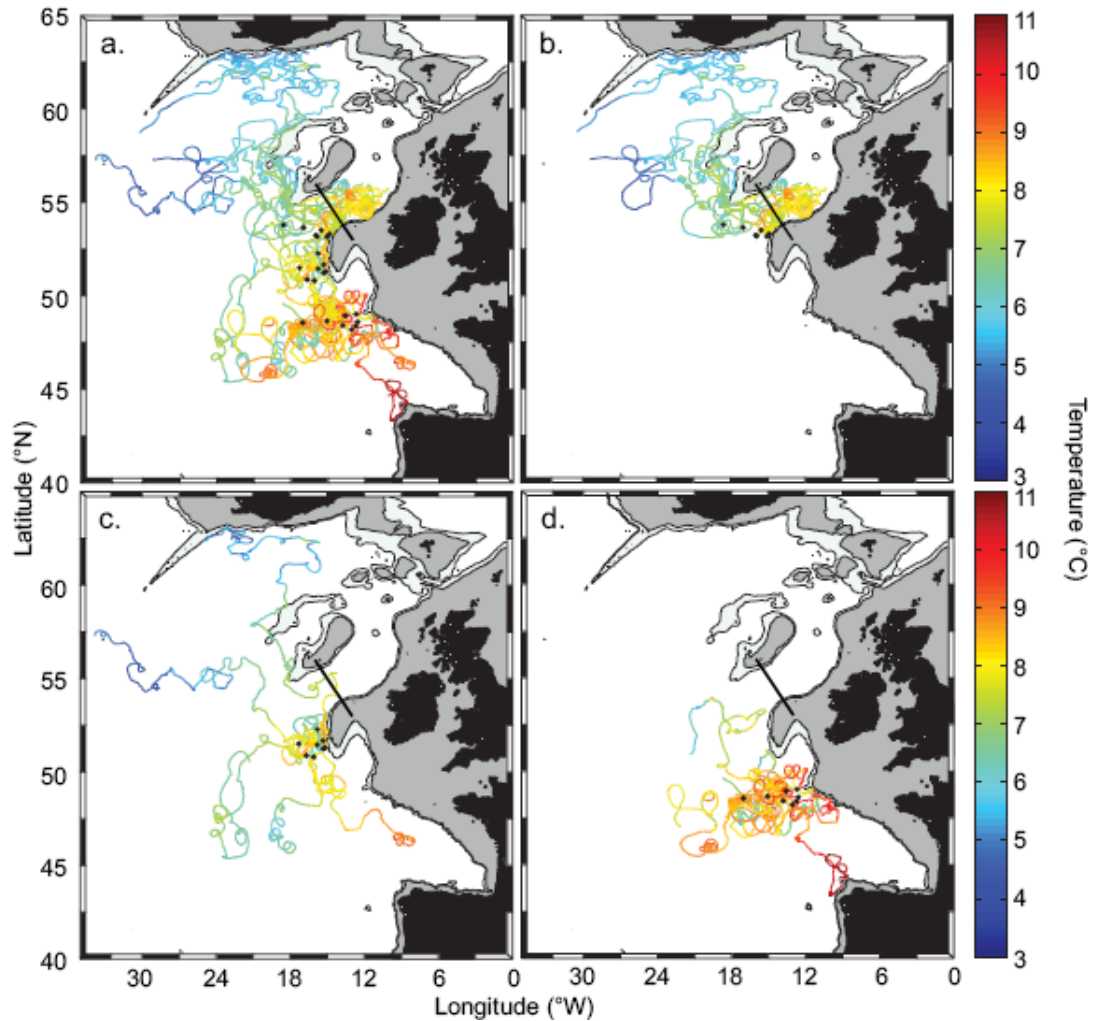


Figure 2: Trajectories of RAFOS floats released between 1996 and 1997 and grouped according to launch position: (a) All floats. (b) Floats launched north of 53°N (c) Floats launched between 50-53°N and (d) Floats launched south of 50°N. In all panels, trajectories are colored by the temperature recorded by the float along its path. Bathymetry is from the 2' resolution ETOPO2 database. 500 and 1000 m contours are shown in gray. Black dots indicate float launch location and black line indicates entry to Rockall Trough.

2.2 Background

A mid-depth current in the eastern North Atlantic was first proposed as an MOW transport pathway by Reid in 1979. Reid hypothesized that an eastern boundary undercurrent, stretching along the western African and European continental shelves, transported MOW northward from the Gulf of Cadiz to the Rockall Trough and on into the Norwegian-Greenland Sea. However, later studies [Arhan *et al.*, 1994; McCartney and Mauritzen, 2001] showed no evidence of Reid's eastern boundary current at high latitudes, calling the role of the current in transporting MOW beyond Porcupine Bank (blue star, Figure 1) into question. Two later studies suggested alternative theories: McCartney and Mauritzen (2001) hypothesized that an eastern boundary current bore no responsibility for carrying MOW to high latitudes at all; instead, they suggested that the high salinity waters entering the Norwegian-Greenland Sea are warm and salty near-surface subtropical waters subducted along the path of the North Atlantic Current (NAC). In a reconciliation of these opposing views, Lozier and Stewart (2008) suggested that the northward penetration of MOW varies with the state of the North Atlantic Oscillation (NAO). Lozier and Stewart hypothesized that during periods when the NAO is consistently low (characterized by weak westerly winds and a zonal contraction of the subpolar gyre [Bersch *et al.*, 1999]), MOW is able to penetrate northward into subpolar waters, resulting in increased salinity anomalies in the Rockall Trough and beyond. Conversely, when the NAO index is high (characterized by strong westerly winds and an eastward shift in the subpolar front), MOW is blocked from penetrating northward by an

eastward migration of the subpolar front, and the salinity signature in the Rockall Trough decreases. The Lozier and Stewart circulation scheme has since been used to describe variability in the properties of waters as far north as 60°N [Sarafanov *et al.*, 2008]. However, though the scheme convincingly linked variability in the northward penetration of MOW to changes in high latitude salinities, the specific pathways by which MOW reaches high latitudes were not detailed.

Both model [Eden and Willebrand, 2001; Brauch and Gerdes, 2005; Deshayes and Frankignoul, 2008] and observational [Bersch *et al.*, 1999; Curry and McCartney, 2001; Flatau *et al.*, 2003; Bersch *et al.*, 2007] evidence has suggested a link between NAO induced atmospheric forcing and circulation changes within the subpolar gyre. The temporal variability in the advection of MOW described by Lozier and Stewart relies on one of those NAO induced changes: namely, a migration in the zonal position of the eastern limb of the subpolar front. This position is impacted by the strength of the westerlies, as measured by the NAO index [Hurrell, 1995]: when the NAO index is high, the atmospheric sea-level pressure difference between the Azores High and the Icelandic Low increases, strengthening the westerly winds. This strengthening is believed to shift the eastern limb of the subpolar front eastward [Bersch *et al.*, 1999]. Because of the strongly barotropic nature of the subpolar gyre, this eastward migration is present throughout the thermocline [Hakkinen and Rhines, 2004]. Lozier and Stewart hypothesize that this migration results in the “blocking” of the northward advection of

MOW at ~1100 m. Conversely, they argue that during a negative NAO state, the zonal winds weaken and the gyre contracts, resulting in a westward shift in the subpolar front.

A recent study [*Häkkinen and Rhines, 2004*] provided an alternative index to the NAO for the quantification of changes in the subpolar gyre circulation. Using satellite-based measurements from 1992 to 2002, *Häkkinen and Rhines* produced an index, later coined the “gyre index”, from the principal component of an empirical orthogonal function (EOF) analysis of sea surface height. During high “gyre-index” years (such as the early 1990s) the eastern limb of the subpolar gyre expands into the eastern subpolar basin and during low “gyre-index” years, the eastern limb of the subpolar front shifts westward [*Hatun et al., 2005*]. As an ocean-based (rather than atmospheric-based) measurement, the gyre index is a better descriptor of the gradual shifts in the position of the eastern limb of the subpolar front than the more frequently fluctuating NAO index. As such, this index will be used in this study to characterize regional circulation changes in the eastern subpolar North Atlantic.

2.3 Data and Methods

Analyses for this study were conducted utilizing Eulerian and Lagrangian data from both the observational record and from an OGCM. The data from the observational record is summarized in Section 2.3.1, followed by a description of model data in Section 2.3.2.

2.3.1 Observational Data

Lagrangian pathways examined in this study resulted from the release of 23 Ranging and Fixing of Sound (RAFOS) floats launched in 1996-1997 as part of the Atlantic Circulation and Climate Experiment (ACCE) [Furey *et al.*, 2001]. As described in Furey *et al.* [2001], all RAFOS floats were ballasted to follow the $\sigma_t = 27.5$ surface in order to target the poleward-flowing eastern boundary current. The RAFOS floats were tracked by sound sources throughout the northeastern North Atlantic (as described in Bower *et al.* [2002]) for two years before resurfacing and transmitting their daily position, temperature and pressure data via satellite.

Salinity anomalies in the Rockall Trough are calculated relative to the climatological average using historical hydrographic data extracted with Hydrobase2 [Lozier *et al.*, 1995; Curry, 1996] and updated with data from the World Ocean Database 2005 [Boyer *et al.*, 2006]. Salinity anomalies within the observational record are calculated along $\sigma_1 = 32.1$, an isopycnal that lies at the core of the MOW tongue at 36°N and used previously in the Lozier and Stewart (2008) analysis. This isopycnal is henceforth referred to as the “MOWobs isopycnal”. All anomalies are calculated in a 5°x5° region within the Rockall Trough (10 - 15°W and 52.5 - 57.5°N), as outlined in Figure 1.

2.3.2 FLAME Data

To complement the data provided by the observational record, this study also utilizes 15 years of output from a realization of the $1/12^\circ$ resolution FLAME ocean general circulation model (Family of Linked Atlantic Model Experiments) [Böning *et al.*, 2006; Biastoch *et al.*, 2008]. FLAME is a z-coordinate model with 45 levels spaced 10 m apart near the surface and 250 m at depth with a gradual transition between those spacings. The horizontal domain of the model is 100°W - 16°E and 18°S - 70°N . Following a 10-year spin-up, the model realization analyzed in this study was forced at the surface with monthly-averaged NCEP/NCAR anomalies superposed on European Center for Medium-Range Weather Forecasts (ECMWF) monthly climatologies. The available model output spans the years 1990-2004 with 3-day temporal resolution.

The isopycnal chosen for the MOW calculations in FLAME is $\sigma_2 = 36.7$, henceforth referred to as the “MOWmod isopycnal”, which resides at ~ 1000 m along much of the eastern basin of the North Atlantic. This σ_2 surface is approximately equivalent in the subpolar eastern North Atlantic to $\sigma_1 = 32.2$, quite close to MOWobs isopycnal. Velocity fields on MOWmod isopycnal exhibit a poleward-flowing current that extends northward from the Strait of Gibraltar, enters and then circulates around the Bay of Biscay. As in observational studies [Ahran *et al.*, 1994; McCartney and Mauritzen, 2001; Iorga and Lozier, 1999a], detection of a coherent current fails beyond Porcupine Bank (blue star in Figure 1). However, despite this lack of detection, the magnitude of subsurface salinity

anomalies in the Rockall Trough are maximized at the depth of the MOWmod isopycnal, suggesting the presence of MOW, in agreement with the observational record (Figure 3). Rockall Trough anomalies from the model output are analyzed along the MOWmod isopycnal averaged over the same $5^\circ \times 5^\circ$ box ($10\text{-}15^\circ\text{W}$, $52.5\text{-}57.5^\circ\text{N}$) used for the analysis of the historical hydrographic data.

In order to complement the RAFOS float pathways, FLAME velocity fields were used to produce synthetic trajectories along the eastern boundary from 2 launch location schemes. Details regarding the computation of these synthetic trajectories are well described in *Gary et al.* [2011] and as such are not reproduced here. In the first launch scheme, launches were initiated from the launch locations of the 23 RAFOS floats. These “synthetic RAFOS launches” were seeded at the local depth of the MOWmod isopycnal and, for consistency with the observational RAFOS floats, allowed to run for 2 years. Furthermore, in order to understand the impact of longer drifter duration, these runs were repeated with drifter lifetimes of 5 years. The floats were advected forward through the model’s 3d velocity fields, with their position, salinity and temperature recorded along their path. Launches from the RAFOS sites were repeated every month between 1990 and 2000 (launches initiated beyond 2000 could not have been run for 5 years since model fields are available only until December, 2004) such that 120 batches of floats were released from the 23 launch locations, for a total of 2,760 floats launched

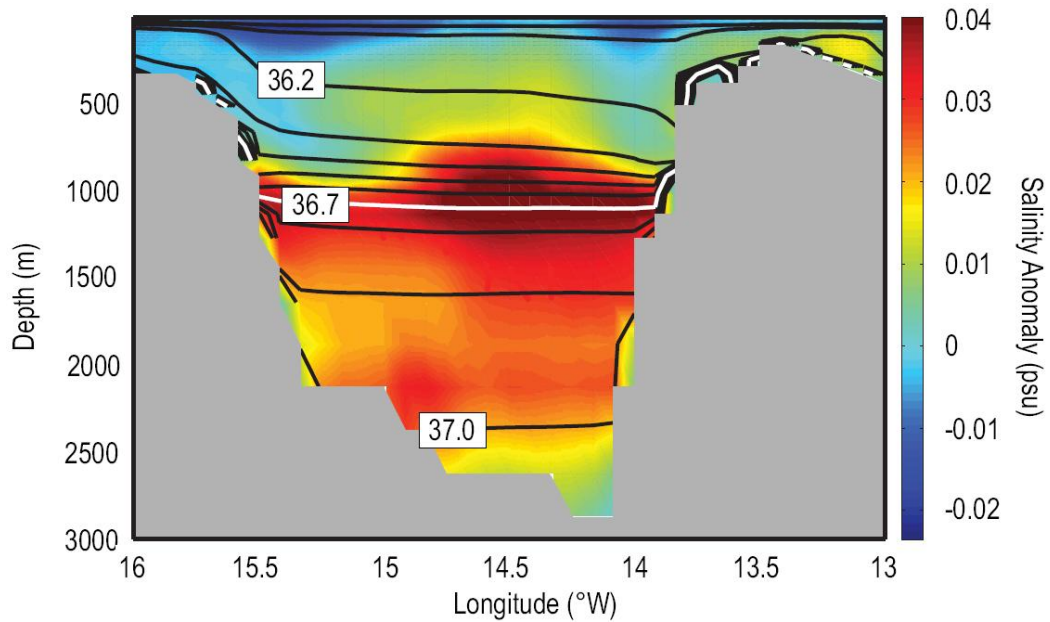


Figure 3: Isopycnal contours (referenced to 2000 db) at the entry of the Rockall Trough shown over the mean subtracted salinity anomalies. Anomalies were calculated as the 2003/2004 salinity fields – 1990-2004 mean salinity fields. The white isopycnal denotes the MOWmod isopycnal, which passes through the core of the positive anomalies in the Trough. Contour interval is 0.1 kg/m^3 . Floats in the Rockall Reverse launch scheme were released between 1000-1150 m in order to approximate the depth of the MOWmod isopycnal. Bathymetry at the entry to the Trough is shown in gray.

over the 10-year period. Results from these launches and from the observational RAFOS floats are used in Section 2.4.1 to elucidate MOW pathways along the eastern boundary.

The second launch scheme (henceforth referred to as the “Rockall Reverse” launch scheme) was designed to investigate the Lagrangian pathways that lead to the subsurface maximum in salinity anomalies along the MOW_{mod} isopycnal in the Rockall Trough. As such, the entry to the Rockall Trough was seeded with floats that were run backwards in time to elucidate the pathways by which they reached the region of high salinity anomalies within the Rockall Trough. The floats were seeded at depths (1000-1150 m) spanning the depth of the MOW_{mod} isopycnal (1050-1100 m) in the Rockall Trough (Figure 3). Floats were seeded such that the number of floats released was proportional to the transport at the launch position at the time of the launch, *i.e.* more floats were seeded into high transport regions than into areas of low transport. In order to provide adequate time for floats to exit the Rockall Trough region, floats were advected backwards in time through the 3d velocity fields for 6 years. To provide a high resolution record of temporal changes in the Lagrangian pathways leading to the subsurface salinity maximum, batches of floats were released from a section across the Rockall Trough every 10 days between 1996 and 2004 (floats launched before 1996 would could not be advected in reverse for their full 6-year lifetime). In total 155,026 Rockall Reverse floats were released. These launches are examined within the context of changes to the subpolar gyre circulation patterns in Section 2.4.3.

2.4 Results and Discussion

The questions posed in Section 2.1 are investigated in turn in this section. We begin with an analysis of MOW pathways in the eastern Atlantic using both RAFOS and synthetic floats. Large scale changes to the subpolar gyre circulation are described in Section 2.4.2 and a description of mean and variable Lagrangian pathways leading to the Rockall Trough is discussed using the “Rockall Reverse” launches in the FLAME model in Section 2.4.3.

2.4.1 What are the pathways that carry MOW to the eastern subpolar gyre?

When taken together, the trajectories and temperatures recorded by the 23 RAFOS floats released along the eastern boundary between 1996-1997 [Figure 2a and *Bower et al.*, 2002] appear to reveal generally northward pathways that are marked by relatively warm temperatures, consistent with the transport of MOW from low to high latitudes. In Figures 2b-d, the trajectories of the RAFOS floats are separated into those launched north of 53°N (7 floats, Figure 2b), between 50-53°N (8 floats, Figure 2c) and south of 50°N (8 floats, Figure 2d). Such division reveals nuances of these pathways: the majority of the RAFOS floats entering the Rockall Trough (5 of 6) originate north of 53°N (Figure 2b) and only one of these high latitude floats remained in the Trough for the duration of its life. Furthermore, none of the floats launched south of 53°N show any clear northward (or southward progression) and none enter the Rockall Trough. The limited number of

floats, the limited 2-year lifetimes and the limited realizations of the flow field (all floats were launched in 2 batches: November/December 1996 and November 1997) preclude firm conclusions on observational MOW pathways, however, it is clear that the pathways yield little support for a spatially continuous current of MOW along the eastern boundary of the North Atlantic. Additionally, these float pathways leave open the question of how MOW reaches the Rockall Trough.

Thus, to study MOW pathways to the subpolar domain, we turn to synthetic floats generated by FLAME velocity fields. In order to provide confidence in the model's ability to produce reasonable trajectories in this region, 2-year trajectories and temperature changes of synthetic floats launched in December of 1996 (chosen to match the launch time of a batch of RAFOS floats) are shown in Figure 4 superposed upon the 2-year trajectories of the RAFOS floats. Though the temperature range sampled by the floats in Figure 4 is slightly narrower than the range sampled by the floats in the observational record, the spatial distribution of the RAFOS synthetic trajectories is a good match with the distribution of floats in the observational record. As such, we next examine the two sets of "synthetic RAFOS launches" discussed in Section 2.3. The percentages of floats that enter the Rockall Trough and the subpolar gyre (as measured by the float crossing the mean position of the line of zero wind stress curl used to force the model) from each of these sets are shown in Table 1.

Table 1: Percent of RAFOS and synthetic floats reaching the Rockall Trough (RT) and subpolar gyre (SP) with lifetimes of 2 and 5 years. Floats are binned by their launch location (high, mid and low latitude). Error estimates come from the standard deviation of the % of floats arriving from different launch locations. One RAFOS float launched at mid-latitudes was lost to the sound sources before surfacing in the Rockall Trough. This float is not included in the estimate of mid-latitude RAFOS floats reaching the RT (denoted by *). Entry into the subpolar gyre was determined by the float crossing the climatological mean position of the zero wind stress curl line from the model forcing fields.

	RAFOS to RT (2 yrs)	FLAME to RT (2 yrs)	FLAME to RT (5 yrs)	FLAME to SP (2 yrs)	FLAME to SP (5 yrs)
HIGH	5/7	33 (± 7) %	37 (± 7) %	70 (± 7) %	83 (± 5) %
MID	1/8*	6 (± 3) %	11 (± 4) %	32 (± 12) %	56 (± 8) %
LOW	0/8	1 (± 1) %	3 (± 2) %	5 (± 5) %	22 (± 7) %

As might be expected from the RAFOS results, Table 1 indicates that a large number (> 50% in all locations) of the floats launched at high latitudes enter the subpolar gyre regardless of their lifetime, likely indicative of floats entrained in the large scale subpolar gyre circulation, as seen with the RAFOS floats (Figure 2b). A relatively high percentage (33%/37%) of the (2-year/5-year) floats at high latitudes also enter the Rockall Trough. Though this percentage is lower than the 71% that entered the Trough in the observational record (5 of 7 floats), the small number of observational floats do not yield a representative sample. However, as in the observational record, the 2-year/5-year floats launched at mid/low latitudes rarely (<11%/<3%) reach the Rockall Trough within five years.

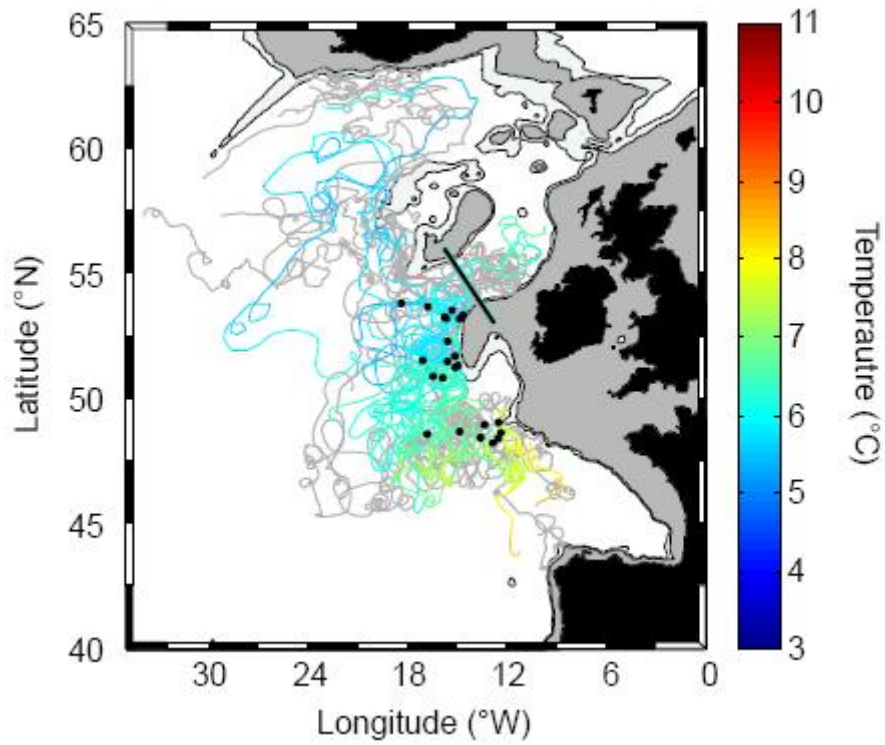


Figure 4: Trajectories of 23 synthetic floats launched in FLAME in December, 1996 from the locations of the RAFOS floats. As in Figure 2, color indicates temperature along the path of the float. Gray trajectories are trajectories of actual RAFOS floats (as in Figure 2a). Black dots indicate launch position. The 500 and 1000 m model bathymetry contours are shown in gray.

This analysis of observational and simulated floats suggests that there is no swift or direct pathway from the eastern North Atlantic to the Rockall Trough region. Thus, the effort to understand the source of the salinity variability at mid-depth in the Trough is better served by investigating the pathways reaching that locale rather than by further investigating pathways that *might* reach that locale. Toward this end, back-trajectories from the Rockall Trough are examined in Section 2.4.3. However, prior to examining these pathways, we first set the stage for the discussion by explaining large scale changes in the subpolar gyre circulation between 1990-2004 and the ability of FLAME to reproduce those changes.

2.4.2 Changing High Latitude Salinities and the Circulation of the Subpolar Gyre

As described in Section 2.2, the strength of the subpolar gyre circulation gradually declined from 1990 to 2004 [*Häkinnen and Rhines, 2004*, updated with data provided by personal communication with Häkinnen]. To investigate the ability of FLAME to reproduce this circulation change, the vertically averaged position of the eastern limb of the subpolar gyre in FLAME was examined at 55°N. The position of the front shifts slowly offshore from ~25°W to ~33°W over the 15-year time series (Figure 5). A comparison of this frontal movement to the *Häkinnen and Rhines* gyre index is quite favorable: a 7-month lag of the frontal movement in the model relative to the gyre index

maximizes the correlation coefficient between the two at $r = 0.875$ ($p < .01$) With no lag, the correlation between the two yields $r = 0.860$ ($p < .01$).

Maps of the salinity field on the MOWmod isopycnal during “high gyre index” and “low gyre index” years further validate FLAME’s ability to reproduce the contraction of the subpolar gyre (Figure 6) between 1990 and 2004. An examination of Figure 6 demonstrates that during high index years (1990/1991 in the model), the shape of the subpolar gyre protrudes strongly into the eastern basin and the salinity front between subtropical and subpolar waters is shown to extend all the way to Porcupine Bank. Conversely, during low gyre index years (2003/2004 in the model) the front shifts westward (Figure 6), presumably allowing subtropical waters to flow northward as described in previous studies [*Holliday, 2003; Hátún et al., 2005; Lozier and Stewart, 2008*]. Finally, the salinity of the waters along the MOWmod isopycnal increased in the Rockall Trough as the subpolar front shifted offshore in FLAME (Figure 7). The magnitude of this increase (~ 0.08 psu) between 1990 and 2004 is similar to the magnitude of the salinity increase in the Rockall Trough measured within the observational record (~ 0.1 psu) over the same period. With the strong comparisons between the property field variability in FLAME and the observational record, we conclude that FLAME represents the regional circulation changes of the subpolar gyre appropriately between 1990 and 2004. As such, we next examine the pathways of waters that enter the Rockall Trough at the depth of the salinity anomaly maximum, investigate the changes in those pathways

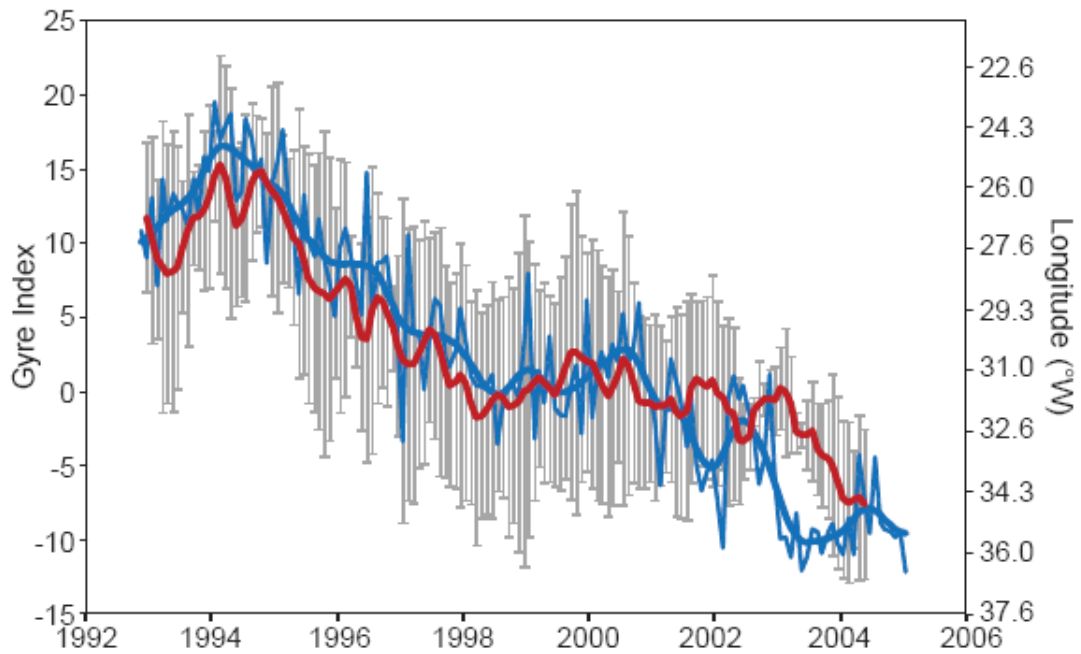


Figure 5: Average zonal shift in the position of the subpolar front at 55°N in FLAME (red), compared with the smoothed Häkkinen and Rhines gyre index (blue). The frontal movement in FLAME was calculated by the zonal position of the 35.0 isohaline on all depth surfaces between 333 meters and 1135 meters and the 34.98 isohaline for 1273 meters (which was utilized to avoid bathymetry). Gray error bars the standard deviation of the calculated frontal position between 333 and 1273 m. Thin blue curve denotes unsmoothed gyre index. FLAME frontal movement was smoothed with a 3-month running mean.

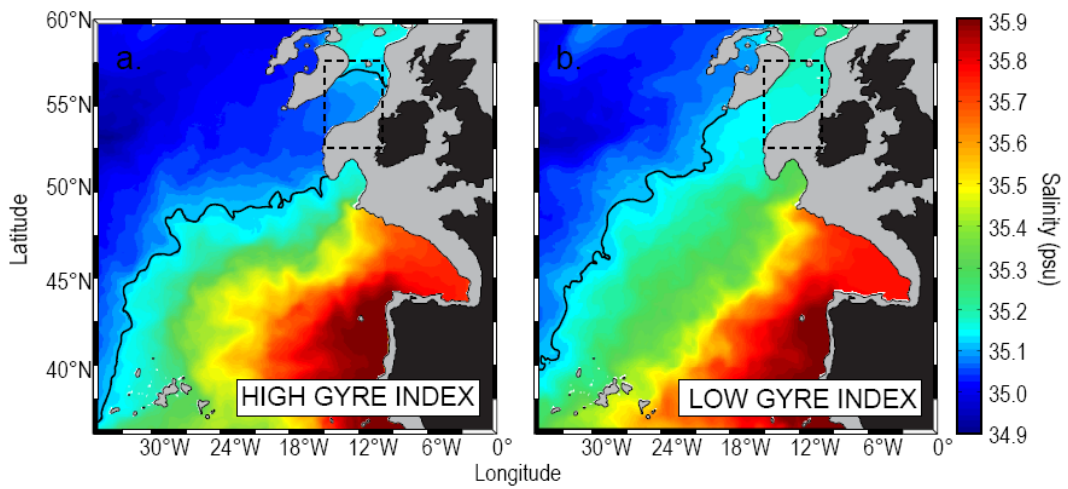


Figure 6: Salinity fields in (a) high (1990-1991) and (b) low (2003-2004) gyre index years along the MOWmod isopycnal in FLAME. Solid black contour indicates the 35.1 psu isohaline and dashed black line indicates the position of the Rockall Trough box used in this study. 1000 m bathymetry contour is shown in gray.

driven by shifts in the regional circulation and determine whether those changes can produce the observed mid-depth salinity increase within the Rockall Trough.

2.4.3 Lagrangian Pathways to the Rockall Trough

In order to elucidate the pathways by which waters enter the Rockall Trough, floats were released from the depth of the mid-depth salinity anomaly in the Rockall Trough as described by the “Rockall Reverse” launch scheme in Section 2.3.2. 100 randomly-selected trajectories from those launches are shown in Figure 8a. Once released from the launch line spanning the entry to the Rockall Trough (dotted line in Figure 8a), the reverse trajectories were analyzed to determine their region of origin. To facilitate this analysis, four lines were chosen to enclose the Rockall Trough (solid lines in Figure 8a): one line spans the eastern North Atlantic (henceforth called the ENA line), another roughly corresponds with the position of the Mid-Atlantic Ridge (the MAR line), another follows the Reykjanes Ridge (the REYK line) and a fourth spans the entry to the Norwegian-Greenland Sea (the Wyville-Thomson Ridge line: WT). Float trajectories in Figure 8a are colored by the line through which they entered the Rockall Trough region: those that enter the Rockall Trough region through the MAR and ENA lines are colored blue and red, respectively. Floats that recirculated within the box defined by the four lines for their entire 6-year lifetime are colored green. In the randomly-selected floats plotted in Figure 8a, no floats entered the Rockall Trough through the REYK and WT lines.

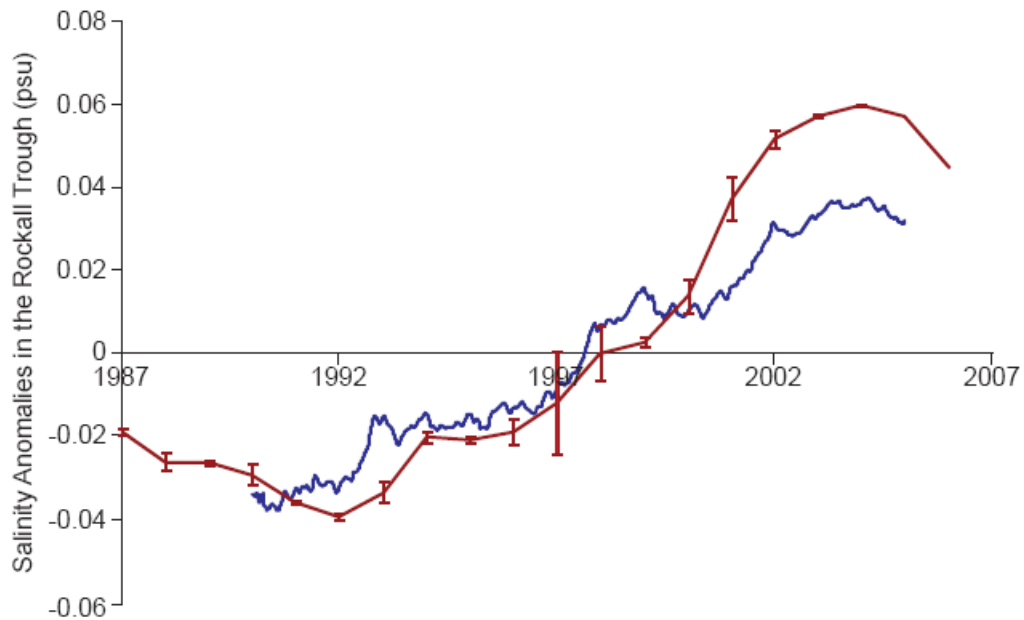


Figure 7: Mean subtracted anomalies in the Rockall Trough along the (blue) MOWmod isopycnal in FLAME and (red) the MOWobs isopycnal in the observational record. Both FLAME and observational data was averaged over the $5^{\circ} \times 5^{\circ}$ RT degree box (shown by dashed lines in Figure 6). FLAME data was collected every 3 days. Observational data consists of yearly averages smoothed with a 5-year running average and error bars indicate standard errors. Because of the large number of data points available for the FLAME timeseries and the high temporal resolution, standard error bars for FLAME are too small to be included in this figure. The slope of the FLAME anomalies was determined to be $0.0053 (\pm 0.00002)$ psu/yr and the slope of the smoothed observational anomalies was determined to be $0.0075 (\pm 0.0007)$ psu/yr.

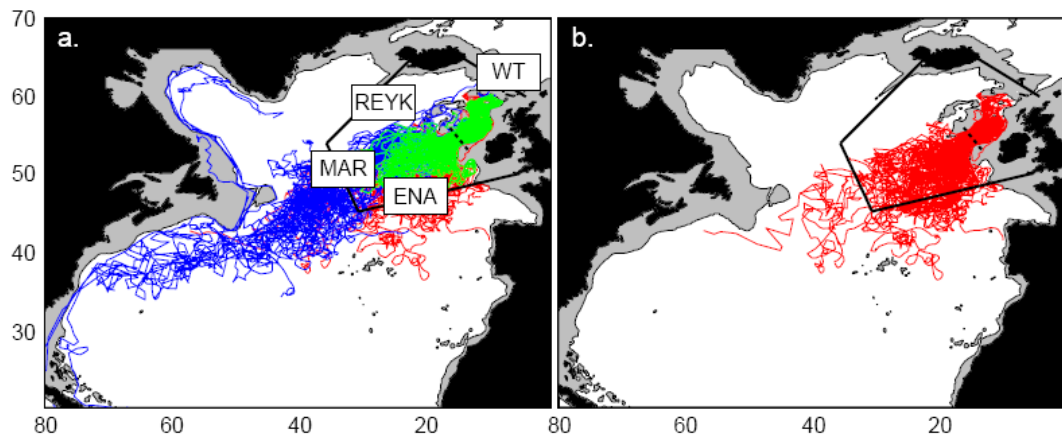


Figure 8: (a) Trajectories of 100 randomly selected floats released from the Rockall Reverse launch positions (along the dashed black line spanning the Rockall Trough) and run backwards in time for 6 years. The trajectories shown are representative of the 155,026 floats released in total. Floats which entered the Rockall Trough through the ENA and MAR lines are shown in red, and blue respectively. 1000 m bathymetry contours are shown in gray. (b) Same as in (a) but with only the ENA floats shown.

As evident by the trajectories in Figure 8a, the two major pathways by which floats enter the Rockall Trough pass through the MAR and ENA lines. Only 1077 (0.69%) and 432 (0.28%) floats entered the Trough through the WT and REYK lines, respectively. 59,139 floats (38.1%) recirculate within the Rockall Trough region for the duration of their lives and hence have no clear origin. As for the major pathways, of the 155,026 floats released, 53,729 (34.7%) and 40,649 (26.2%) entered the Rockall Trough region through the MAR and ENA lines, respectively. For clarity, the floats that entered through the ENA line are shown plotted separately in Figure 8b. As evident by their trajectories, some of the floats (13.0%) that enter the RT through the ENA actually originate in the western subtropical gyre and are carried by the NAC into the eastern North Atlantic. However, because they passed through the MOW reservoir before flowing northward through the ENA line, those floats are considered ENA floats for the purpose of this analysis. These “hybrid-pathway” floats reveal the limits on our ability to clearly distinguish a pathway as either ENA or MAR: though we treat the two lines as separate entry points to the Rockall Trough, the trajectories in the eastern North Atlantic reveal a continuum of pathways that stretch from the relatively fresh NAC to the saltier MOW waters of the eastern North Atlantic. However, as explained below, these two defined origins do allow us to distinguish between Lagrangian pathways that bring relatively fresh or relatively salty water to the Rockall Trough. Thus they provide a useful, albeit imperfect, tool for this analysis.

To describe the 3d pathways by which floats reach the entry to the Trough, floats that passed through the MAR and ENA lines were binned by depth as well as latitude or longitude (Figure 9a). The spatial distribution in Figure 9a highlights a number of features. In both the MAR and ENA panels, the majority of floats that enter the Rockall Trough are near the MOWmod density surface at their upstream position. The trace of this isopycnal along the MAR and ENA lines is shown by the white line in Figure 9a. Most of the floats entering the Rockall Trough originate along the MAR line at the depth of the MOWmod isopycnal, presumably carried to the Trough by the NAC. However, a significant number of floats originate along the ENA at the depth of the MOWmod isopycnal. Additionally, some floats followed the pathway hypothesized by *McCartney and Mauritzen*, subducting along the path of the NAC until they reach the Rockall Trough. As suggested by McCartney and Mauritzen, the salinities and temperatures of these shallow subtropical waters at the MAR line indicate that they are a source of both heat and salt to the Rockall Trough. However, these shallow floats account for only 3.9% of the total floats entering the Trough and as such are unlikely to make a significant contribution to property field variability when compared with the much larger influence of the flow along the MOWmod isopycnal. In Figure 9b, the outline of the area with the highest concentration of floats (100 floats/km²) that reach the Rockall Trough from the MAR and ENA lines is superposed on the salinity anomalies along those lines: the salinity anomaly is calculated as the climatological salinity at the line minus the climatological salinity of the Rockall Trough. As apparent by the outlined regions in Figure 9b, floats that pass through the MAR line largely supply fresh water to the RT

whereas floats passing through the ENA line supply salty water. Thus, a circulation change that brings more NAC waters to the RT would be expected to decrease the salinity in the vicinity of the RT, while a change that brings more ENA water would cause a salinity increase.

Overall, the results from Figure 9 indicate that density neutral pathways through the MAR and ENA lines are largely responsible for supplying fresh and salty waters, respectively, to the depth of the subsurface maximum in salinity anomalies within the Rockall Trough. Left unresolved is whether changes in these pathways, particularly within the framework of shifting subpolar gyre circulation patterns, could explain the increase in subsurface salinities along the MOW_{mod} isopycnal in the Rockall Trough between 1990 and 2004. In order to investigate this question, floats were launched repeatedly from RT to quantify the interannual variability of the two major pathways. As shown in Figure 10, the number of floats arriving in the Rockall Trough through the MAR line decreased annually by 0.6 (± 0.08) % with a total decrease of $\sim 5.4\%$ between 1996 and 2004 while the number of floats arriving from the eastern North Atlantic through the ENA line increased annually by 1.2 (± 0.09) %, for a total increase of $\sim 11.2\%$ over the same period. This shift in the number of floats arriving from each pathway is consistent with the expectation based on the gyre dynamics described in Section 2.4.2: as the subpolar gyre contracts between 1990 and 2004 and the eastern limb of the subpolar front moves westward, more water from the eastern North Atlantic is able to penetrate to

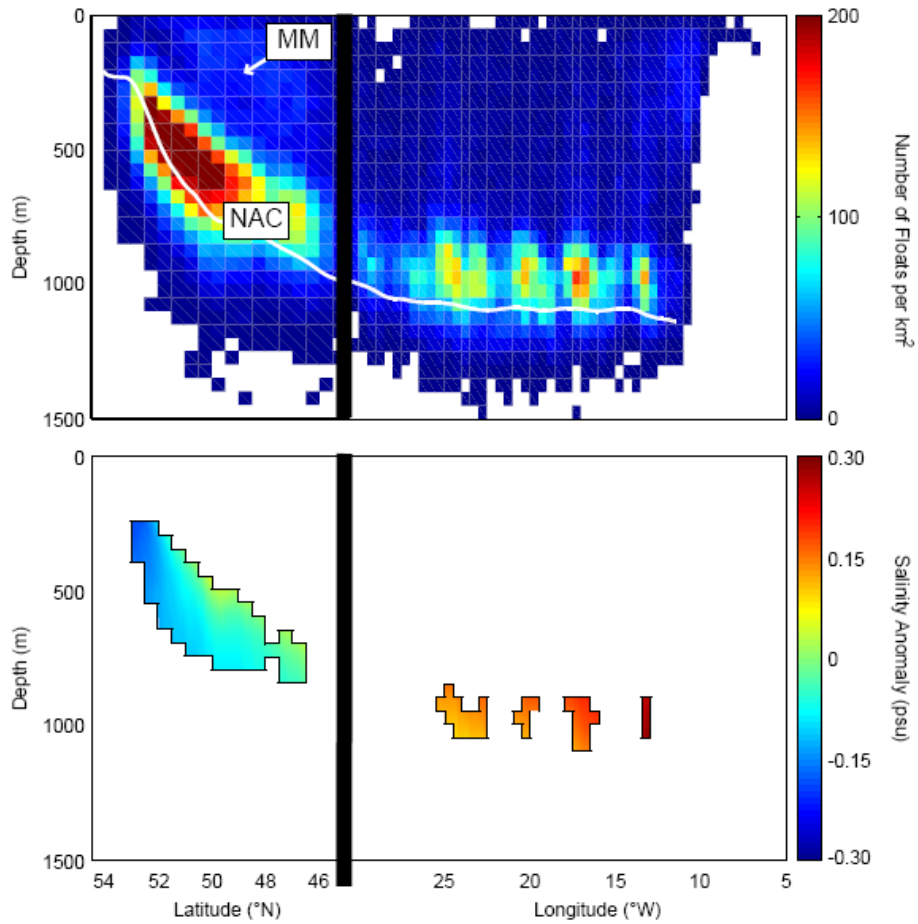


Figure 9: (top) Number of floats (per m^2) released from the Rockall Trough launch line which passed through the MAR (left) and ENA (right) launch lines. Bin sizes were $1/2^\circ$ latitude (left) and $1/2^\circ$ longitude (right) \times 50 m. MM denotes McCartney and Mauritzen water and NAC indicates North Atlantic Current water. White line indicates the climatological position of the MOWmod isopycnal along the MAR and ENA launch lines. (bottom) Contour of the location through which > 100 floats/ km^2 arrive in at the MAR and ENA launch lines superposed over climatological salinity anomalies (relative to the salinity in the Rockall Trough) along the lines.

high latitudes. It therefore follows that over this time period the influence of the NAC on water properties in the Rockall Trough decreases.

Figure 10 also indicates that there is a statistically significant drop ($0.8 (\pm 1) \%$ /yr) in the number of recirculated floats entering the Rockall Trough over the time period of interest, resulting in a total drop of $\sim 7.2\%$ between 1996 and 2004. Thus, it appears that the long term advance of ENA waters towards the Rockall Trough acts to flush the recirculating waters from the Rockall Trough region, filling it instead with warmer, saltier waters of eastern Atlantic origin. Such flushing apparently also occurs on interannual time scales in response to changes in the amount of MAR and ENA waters that reach the Trough. The correlation between changes in the numbers of ENA and recirculated floats is -0.78 ($p < 0.01$) over the time period of interest, while the correlation between changes in the number of MAR and recirculated floats is -0.53 ($p < 0.01$). Thus, as more (less) waters advance into the Rockall Trough from either the MAR or ENA lines, fewer (more) waters are locally recirculated. Interestingly, but perhaps not surprisingly, despite the strong correlation between the ENA and recirculated waters, and that between the MAR and recirculated waters, the correlation between changes in ENA and MAR floats is not statistically significant. Instead, it appears as though there is a reservoir of eastern subpolar North Atlantic water that resides outside the Rockall Trough that provides essentially a buffer for changes in salinity to the area brought about by changing pathways, themselves a result of the regional circulation changes described in Section 2.4.2.

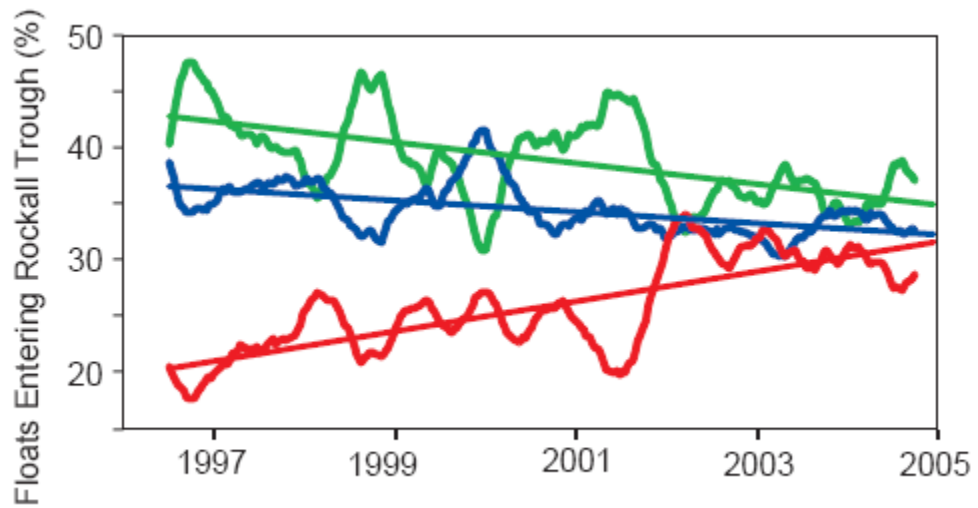


Figure 10: Percent of floats arriving in the Rockall Trough through the (blue) MAR and (red) ENA lines as well as those that were (green) recirculated within the Rockall region throughout their lives. A 6-month running mean was used to smooth all curves.

2.5 Summary

The evolution of subsurface salinity anomalies within the Rockall Trough has been the focal point of several studies over the past few years. Eulerian investigations of both observed and modeled salinity and velocity fields have concluded that NAO-induced changes to regional circulation patterns (specifically, to the zonal position of the eastern limb of the subpolar gyre) were the likely cause of the anomalies. However, questions remained about the nature of the Lagrangian pathways that carried the MOW and other subtropical waters into the Rockall Trough.

Synthetic floats launched backwards in time from a line spanning the entry to the Rockall Trough at the depth of the subsurface salinity maximum indicate that the two main transport pathways leading to the Rockall Trough are (1) relatively fresh waters transported along the MOW_{mod} isopycnal as part of the North Atlantic Current and (2) relatively salty waters transported northward along the MOW_{mod} isopycnal within the eastern North Atlantic, both of which reside within a continuum of waters stretching along a density surface between the NAC and the saltier, MOW-influenced eastern North Atlantic waters. By focusing on two broadly defined pathways in this study, we were able to demonstrate that changes to the regional circulation of the subpolar gyre shift this continuum westward such that a greater amount of salty MOW-influenced eastern North Atlantic waters reach the Rockall Trough as the subpolar front shifts offshore. As such, our Lagrangian results are consistent with previous Eulerian studies of high latitude

property fields, confirming the role of regional circulation changes in establishing high latitude salinities [*Holliday, 2003; Hátún et al., 2005; Lozier and Stewart, 2008*].

Finally, we note that the Lagrangian pathways simulated in this study, as well as the those from the limited observational set, give little indication of the coherent, poleward-flowing eastern boundary current revealed by Eulerian averages from observational and modeling data. Instead, the pathways reveal an eastern North Atlantic flow field with strong temporal and spatial variability: only in the aggregate do the pathways reveal a slow northward progression of MOW. In this way, the North Atlantic eastern boundary current is not unlike its western counterpart where a vibrant eddy field entrains and detrains fluid from the boundary current, thereby greatly increasing the transit time from an upstream to a downstream locale.

3. Subtropical to Subpolar Pathways in the North Atlantic: Deductions from Lagrangian Trajectories

3.1 Introduction

The traditional ‘conveyor belt’ paradigm depicts the meridional overturning circulation in simplistic terms: warm surface waters transported to high latitude regions of deep convection cool and sink, then follow subsurface pathways equatorward until they upwell to the surface and return to high latitudes [*Stommel, 1953; Gordon, 1986*]. It is generally understood that the surface limb of this overturning circulation transports warm surface waters via the Gulf Stream (GS) and North Atlantic Current (NAC) in a continuous path from the subtropical to the subpolar basin, an image supported by the visual connectivity between the mean surface velocity and sea surface temperature fields of the North Atlantic (as seen in model fields shown in Figure 11a and 11b). Estimates of the magnitude of this subtropical to subpolar throughput range from ~13 to 20 Sv [*Hall and Bryden, 1982; Roemmich and Wunsch, 1985; Gordon, 1986; Schmitz and McCartney, 1993; Ganachaud, 2003; Cunningham et al., 2007; Willis, 2010*], which is roughly 20-25% of the overall transport by the upper layers of the Gulf Stream [*Brambilla and Talley, 2006, henceforth BT*]. However, though the concept of a strong and continuous transport of surface waters from the GS to the NAC appears robust in the mean fields, Lagrangian depictions of the GS/NAC system suggest a much weaker connection between the two currents. In their study of North Atlantic surface drifters that passed

through a box surrounding the GS's seaward extension (78-48° W, 35-47°N), BT revealed a lack of connectivity between the subtropical and subpolar basins: though 273 drifters passed through the GS box between 1990 and 2002, only 1 entered the subpolar gyre. A later study of the subtropical to subpolar exchange [*Hakkinen and Rhines, 2009*: henceforth HR] included surface drifter launches through 2007 with similar results: though HR reported an increase in the number of subtropical drifters reaching the subpolar region between 2002 and 2007, the number that reached 53°N (3%) was still far below the number expected to reach the subpolar gyre based on expectations of a strong surface throughput. To explore further the apparent lack of connectivity between the surface waters of the Gulf Stream and those of the eastern subpolar gyre, this study analyzes synthetic drifters launched in an ocean general circulation model (OGCM). Background for this study is presented in the following section, the model used for this study and a description of the methods used for analysis are described in Section 3.3, results follow in Section 3.4, and a summary and concluding remarks are presented in Section 3.5.

3.2 Background

In their exploration of the limited intergyre exchange exhibited by surface drifters, BT offered four hypotheses as to why so few drifters were transported to high latitudes by the GS/NAC system: (1) limited drifter coverage and short drifter lifetimes could have biased the observed amount of exchange, (2) the net southward Ekman transport induced by the

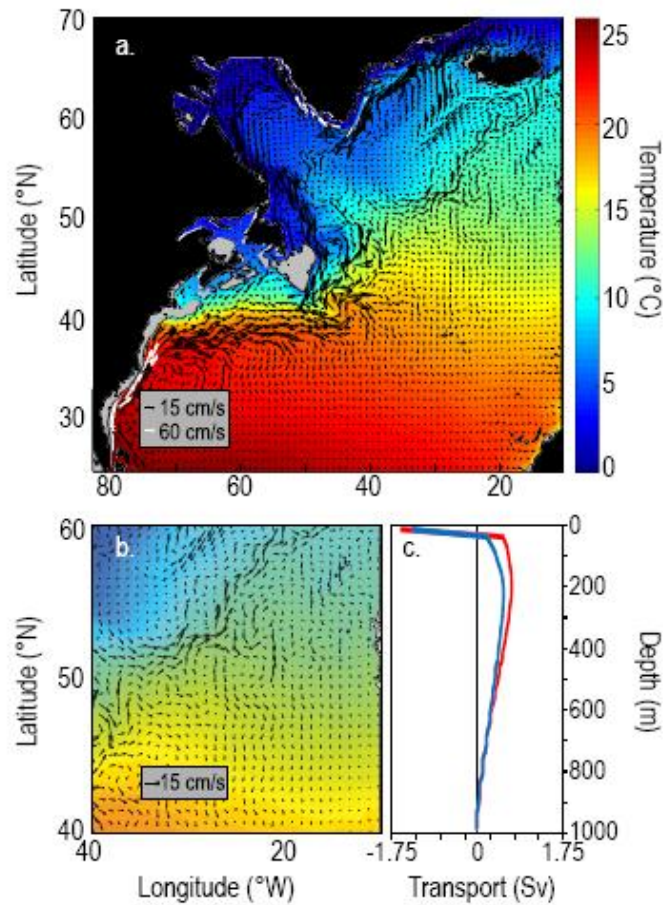


Figure 11: (a) Mean velocity field superposed on the mean temperature field at 15 m in FLAME. Temperature is shown at the full $1/12^\circ$ resolution while velocity is averaged in $1^\circ \times 1^\circ$ bins. Velocities greater than 50 cm/s are shown by white arrows; all other velocities are shown in black. Bathymetry less than 100 m is shaded gray. (b) As in (a) but zoomed in to highlight velocities and temperatures in the northeastern North Atlantic. (c) Mean zonally-averaged meridional transport between (red) $40\text{-}50^\circ\text{N}$ and (blue) $52\text{-}54^\circ\text{N}$ in FLAME. Transports are calculated in 25 m intervals. Total transport over the upper 1000 m between $40\text{-}50^\circ\text{N}$ and at 53°N are 13.0 Sv and 9.8 Sv respectively.

strong westerly winds in the region could have restricted the northward transport of the drifters as they neared the subpolar gyre, (3) the drifters, restricted to 15 m and thus prevented from following the true 3d pathways which occur near the frontal zone at the intergyre boundary [*Qiu and Huang, 1995*], may not have accurately measured the true intergyre exchange, and (4) drifters could have been biased by a preferential inclusion in cyclonic eddies. As described below, the first two hypotheses were tested by BT. In Section 3.4, we will address the third hypothesis. Though the fourth hypothesis will not be explicitly examined in this paper, it should be noted that the OGCM used in this study is fully eddy-resolving and hence contains both cyclonic and anticyclonic eddies in the region of the Gulf Stream. As described in Section 3.3, care is taken in all model tests to ensure that bias based on launch location is removed.

BT calculated the mean lifetime of drifters in the observational record to be 271 ± 260 days, far short of their estimate (400-500 days) of the time required for a drifter launched in the Gulf Stream region to reach the Iceland basin. BT studied the effect of such a short drifter lifetime using examinations of both observational and synthetic trajectories. In one test, BT linked observed trajectories end-to-end until their combined lifetimes totaled more than 600 days. With 600-day lifetimes, 4-5% of linked drifters reached the subpolar gyre. In a second examination, BT launched synthetic drifters in the area bounded by $78-48^\circ\text{W}$ and $35-47^\circ\text{N}$ and then advected the drifters forward in time using both mean and turbulent velocity fields. Their mean surface velocity field was constructed using surface drifter trajectories averaged in $1/2^\circ$ bins over the period 1990-

2002. A time-varying field was created from this mean field by adding a turbulent velocity component for each bin that was calculated from the standard deviation of the velocity for that bin. Advection of the drifters through the mean (turbulent) field resulted in 1% (6%) of drifters reaching the subpolar gyre after three years, a slight increase relative to the 1/273 drifters reaching 53°N with realistic lifetimes in the observational record.

Advection through the mean and turbulent velocity fields was also used by BT to examine the effect of Ekman drift on the number of drifters reaching the subpolar gyre. By removing the Ekman component of the mean (turbulent) velocity field, BT noted an increase in the amount of intergyre exchange by 5% (6%). Interestingly, the ~5% decrease of intergyre exchange related to Ekman drift was found to be roughly proportional to the increase in intergyre exchange resulting from adding a turbulent component to the velocity field (~5%).

In their study of surface drifter trajectories between 1990 and 2007, HR offered another explanation for the small number of surface drifters observed to reach high latitudes in the BT study. Following on the work of *Rhines and Schopp* [1991], HR proposed that the zero of the wind stress curl, a dynamical boundary between the subtropical and subpolar gyres, dictated the extent to which subtropical drifters were able to penetrate into high latitude waters: when the line of zero wind stress curl was essentially zonal, it created a boundary that impeded the northward progress of surface drifters. Conversely, when the

line increased its meridional tilt, it allowed for an expansion of the subtropical gyre into the northeastern Atlantic and essentially connected the Gulf Stream area and the entry to the Nordic Seas. HR concluded that this connection represented a new pathway for subtropical waters to reach high latitudes and suggested that the opening of this pathway was responsible for the observed increase in the number of drifters transported from the “Gulf Stream Box” to 53°N between 1991 and 2007, albeit from only 1/101 (1%) to 8/270 (3%). Though the number of surface drifters reaching high latitudes was small even when the pathway was open, these results raise the possibility that the small amount of exchange measured by drifters in the 1990s and early 2000s was not representative of the “true” intergyre exchange at the surface, but was rather a snapshot of a temporally variable system.

In summary, the small amount of subtropical to subpolar exchange indicated by North Atlantic surface drifters has previously been linked to an underestimate caused by short drifter lifetime and/or a dynamical constraint imposed by Ekman drift. Additionally, it has been suggested that the amount of subtropical waters reaching high latitudes is temporally variable due to shifts in the wind field. Left unexplored from the observational studies of BT and HR are the possible bias in intergyre exchange introduced by drifter launch locations and the possible bias introduced by the drifters’ inability to move in 3d. To examine these possibilities, we analyze synthetic trajectories produced from an eddy-resolving general circulation model. Though the model is not a substitute for the actual drifter-observed exchange, it can be used to place these rather

sparse measurements in context. Furthermore, the model affords the opportunity to examine subsurface pathways of exchange.

Two fundamental questions will be addressed with this study: (1) Can surface drifters from the observational record provide an accurate assessment of surface intergyre exchange and its temporal variability? and (2) Is the amount of intergyre exchange at the surface representative of the overall subtropical to subpolar exchange? With this second question, we stress that our intent is not to suggest or establish the absolute Lagrangian exchange that would be congruent with Eulerian measures, but rather to investigate the depth dependence of intergyre exchange in a Lagrangian framework.

3.3 Methods

This study utilizes 15 years of output from a realization of the $1/12^\circ$ resolution FLAME ocean general circulation model (Family of Linked Atlantic Model Experiments) [Böning *et al.*, 2006; Biastoch *et al.*, 2008]. FLAME has 45 z -coordinate vertical levels spaced 10 m apart near the surface that spread to a maximum spacing of 250 m at depth. The horizontal bounds of the model are 100°W - 16°E and 18°S - 70°N . Following a 10-year spin-up, the particular model realization analyzed in this study was forced at the surface with monthly-averaged NCEP/NCAR anomalies superposed on European Center for Medium-Range Weather Forecasts (ECMWF) monthly climatologies. The available model output spans the years 1990-2004 with 3-day temporal resolution.

A comparison of the mean surface velocity field from FLAME with that calculated from North Atlantic surface drifters [*Fratantoni, 2001; Brambilla and Talley, 2006; Flatau et al., 2003*] demonstrates that FLAME gives a reasonable representation of the surface circulation of the North Atlantic. Mean velocities at 15 m in the model (Figures 11a and 11b) recreate the major surface circulation features measured by drifters, including a strong Gulf Stream with peak velocities in excess of 2 m/s and a retroflection in the northwest corner of the NAC ($\sim 40^{\circ}\text{W}$, 50°N). Furthermore, mean zonally-averaged meridional transports between $40\text{-}50^{\circ}\text{N}$ and between $52\text{-}54^{\circ}\text{N}$ (Figure 11c) total 13.0 and 9.8 Sv respectively in the upper 1000 m which, as described previously, falls within the range (13-20 Sv) of observational estimates. Mean EKE fields at 15 m from FLAME also compare favorably with EKE fields calculated from altimetry data and surface drifter velocity fields [*Fratantoni, 2001* and Figure 12]. Though small differences exist between the FLAME EKE fields and those of either observational measure, those differences are the same order of magnitude as the differences between the two observational records themselves. As such, we conclude that FLAME gives a reasonable representation of near surface circulation and can be considered a reliable tool for this analysis.

In this study, FLAME velocity fields are used to produce synthetic trajectories from two launch location schemes, shown in Figure 13. Details regarding the computation of these synthetic trajectories are described in *Gary et al. [2011]* and as such are not reproduced

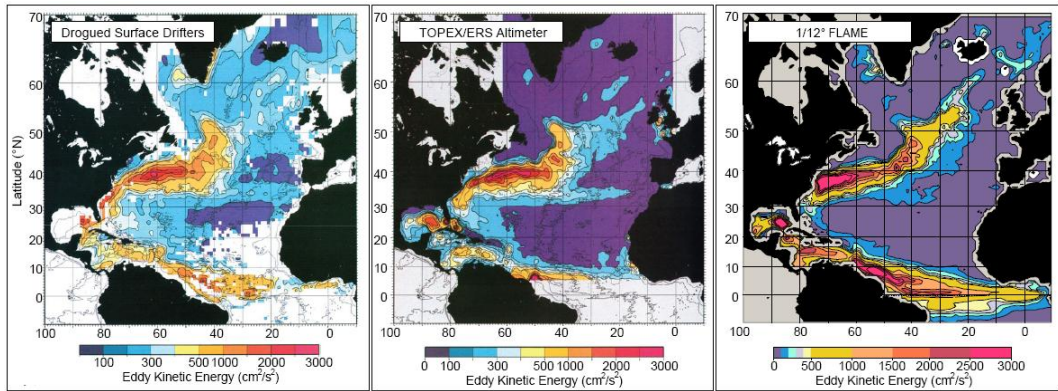


Figure 12: Comparison of EKE fields from surface drifters and satellite measurements with the EKE field from FLAME. All EKE fields were calculated using $1^\circ \times 1^\circ$ bins. Altimeter data analyzed in Fratantoni (2001) were averaged over 1992-1998 and calculated from the geostrophic velocity field. Drifter and FLAME EKE fields were averaged over 1990-1999 and calculated from the full velocity fields. The Ekman contribution to the drifter derived EKE fields was estimated to be less than $20 \text{ cm}^2/\text{s}^2$ over the entire North Atlantic [Ducet *et al.*, 1999]. Drifter and satellite fields are reproduced from Fratantoni (2001) by permission of the American Geophysical Union.

here. The first launch scheme, hereafter referred to as the “observational launch scheme”, consists of drifter launch locations extracted from the NOAA/AOML Global Lagrangian Drifting Buoy Database south of 45°N (Figure 13a). The set of launch locations from 1990-2002 matches those used by BT; the set from 1991-2007 matches those used by HR. Unless otherwise noted, synthetic drifters at these locations are launched at 15 m in order to compare with the drifters in the observational record that were drogued to 15 m to prevent wind slippage [Niiler *et al.*, 1995; Pazan and Niiler, 2001]. For the second launch scheme (referred to as the “Gulf Stream grid”) drifters are spread at 1/2° intervals within the Gulf Stream box (78-48°W, 35-47°N) utilized in the studies of BT and HR. However, to ensure that only subtropical drifters are included in this launch, a dynamical launch strategy is employed. Drifters are launched within this box only if they are located south of the Gulf Stream front, as defined by the position of the 15°C isotherm at 200 m [Fuglister and Voorhis, 1965] on the day of the launch. Thus, the launch pattern is temporally variable; one such pattern is depicted in 13b. Finally, drifters launched with the two sampling schemes described above are considered to have entered the subpolar region when they cross 53°N. The high latitude position of this boundary was chosen for consistency with previous studies [BT, 2006; HR, 2009] and to ensure that floats carried northward to subpolar latitudes are not mistakenly counted as “subpolar” prior to recirculating back to low latitudes. As will be shown in the next section, an inconsequential number of floats return to the subtropical gyre after crossing this latitude. Finally, we emphasize that our intent is to study how waters of subtropical origin reach the subpolar region. Toward that end, we consider cross-gyre

exchange to have occurred when waters of subtropical origin reach the subpolar latitudes. Though some *cross-frontal* exchange may take place as part of this transformation, we are not strictly analyzing the movement of floats or water parcels across a front.

3.4 Results

In this section each of the questions posed in Section 3.2 is investigated in turn within the context of the FLAME model.

3.4.1 Can surface drifters from the observational record provide an accurate assessment of surface intergyre exchange and its temporal variability?

In this section, we use synthetic launches in FLAME to assess the ability of drifters within the observational record to accurately represent the amount of subtropical to subpolar gyre exchange at the surface. In particular, the effects of (1) variable launch location, (2) the constraint of drifter movement to a 2d surface and (3) the effect of Ekman drift are considered. In short, we demonstrate in Sections 3.4.1.1 and 3.4.1.2 that the observational drifters, limited by their variable launch locations and inability to move in 3d, are incapable of representing the nature of subtropical to subpolar gyre exchange. However, prior to addressing these three effects, we first assess exchange similarity between synthetic and observational drifters at 15 m and reexamine the impact of short drifter lifetime on intergyre exchange within FLAME previously investigated by BT.

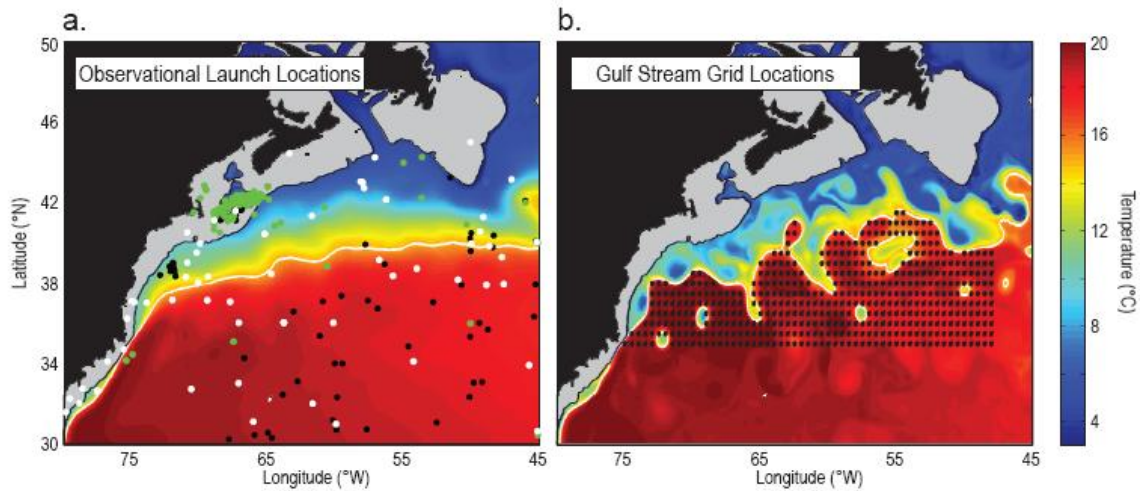


Figure 13: (a) Launch locations of observational drifters in the northwestern subtropical gyre superposed on the climatological mean temperature field at 200 m in FLAME. Black, green and white dots indicate drifters launched between 1991-1995, 1996-2000 and 2001-2005, respectively. White line indicates the climatological position of the 15°C isotherm at 200 m. (b) Sample launch locations of drifters launched within the “Gulf Stream Grid” launching scheme superposed over the temperature field at 200 m at the time of the launch. White line indicates the position of the 15°C isotherm at the time of the launch. In both plots, bathymetry less than 200 m is shaded gray.

Our aim in repeating BT's analysis is to provide some model validation and to set the context for the following analyses. To that end, synthetic drifters were launched from the observational launch locations of three HR pentads (1991-1995, 1996-2000 and 2001-2005) and integrated forward through the time-varying 15 m horizontal velocity fields for 4 years. As seen in Figure 14, despite lifetimes of 4 years, these synthetic drifters exhibit very little intergyre exchange regardless of launch location or forcing. In fact, less than 2.5% of drifters reach 53°N within four years in all pentads (Figure 14), consistent with the results of BT and HR where minimal exchange was found. A more direct comparison with the results of BT is given by the statistics of synthetic trajectories with 600-day lifetimes, where less than 1.1% of drifters reach 53°N in all pentads. This exchange is slightly smaller than the amount of intergyre exchange of the 600-day drifters in the BT study (4-5%), however the difference is likely due in part to the artificial linkage of trajectories separated in both space and time by BT. However, though small differences exist, the conclusion reached by this simple modeling experiment is the same as that reached by BT: though short drifter lifetime may cause a slight underestimation of the amount of intergyre exchange at 15 m, the degree of connectivity between the surface waters in the subtropical and subpolar gyres appears to be small.

3.4.1.1 What are the effects of variable launch locations and the constraint of drifter movement to a 2d surface on the measure of intergyre exchange?

Synthetic drifters are next used to examine the possibility that the drifter-observed exchange is biased by variability in launch location and that indications of temporal variability in that exchange are likewise biased. HR concluded from changes in surface drifter trajectories between 1990 and 2007 that a new subtropical to subpolar pathway had opened, allowing increasing amounts of subtropical water to reach the subpolar basin. However, the surface drifters considered by HR had varying launch locations, which may have artificially increased or decreased the amount of exchange measured from one HR pentad to the next. Specifically, in the HR study, subtropical drifters were defined either by passage through a box surrounding the Gulf Stream (35° - 47° N, 78° - 48° W) or by their low latitude launch location (south of 45° N). Each of these definitions encloses a large region north of the Gulf Stream where subpolar waters are recirculated [Hogg *et al.*, 1986]. As evident in Figure 13a, a number of drifters in the observational data set were not launched in subtropical waters, but instead launched in the recirculation gyre located north of the Gulf Stream front. Drifters launched north of the Gulf Stream would not need to cross the Gulf Stream/North Atlantic Current front in order to reach 53° N, and as a result, may have biased the amount of measured exchange [Lozier and Riser, 1990; Bower and Lozier, 1994].

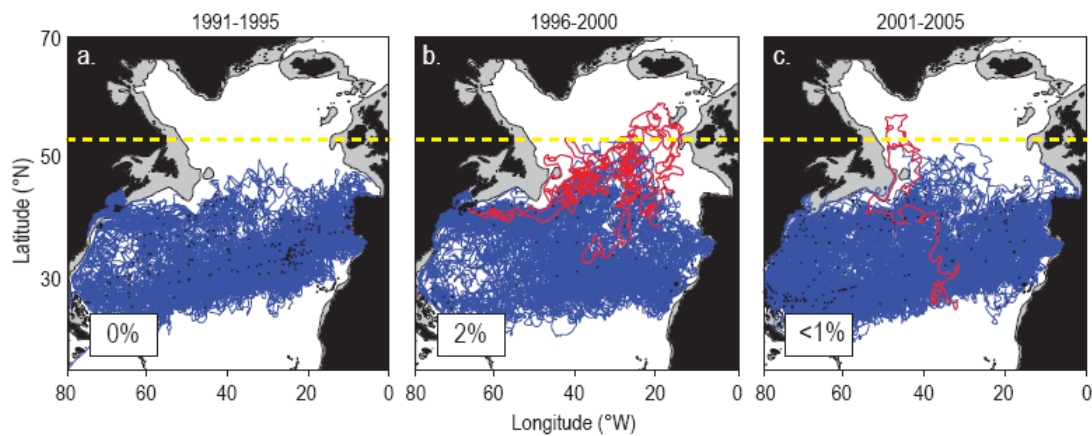


Figure 14: Synthetic drifters launched in FLAME at the observational launch locations (Figure 13a) for each of the three HR pentads (a) 1991-1995, (b) 1996-2000 and (c) 2001-2005 and advected through the instantaneous 15 m horizontal velocity fields from that pentad for 4 years. Transport values at 53°N for the three HR pentads are 10.35, 9.96 and 9.13 Sv respectively. Red trajectories indicate those that crossed 53°N (yellow line). Blue trajectories indicate drifters that remained south of 53°N . The percentage of drifters crossing 53°N is indicated in the white box. Bathymetry less than 500 m is shaded gray.

To examine whether the attribution of temporally variable exchange could be biased by variable launch locations, synthetic drifters were launched from the observational launch locations at 15 m for each HR pentad and then advected through the horizontal velocity field for each pentad for four years. In other words, nine cases were run: drifters were initialized at the launch locations for pentad 1 and then advected forward using the velocity fields for pentads 1, 2 and 3 to yield three measures of intergyre exchange. The launch locations for pentads 2 and 3 were similarly tested. The amount of exchange measured by the surface drifters within each of these nine scenarios is shown in Table 2. Notably, regardless of launch location or forcing, only a small amount of exchange was measured. However, Table 2 indicates that variability in launch location is able to produce as much variability in the amount of exchange measured as variability in the velocity fields through which the drifters are advected (2.3% and 1.9%, respectively). This finding suggests that the variability in the amount of intergyre exchange previously attributed to temporal variability in drifter pathways could just as easily be attributed to variability in drifter launch location. When drifters from the same launch locations are launched through changing velocity fields (as shown by the rows in Table 2), no trend in the amount of exchange can be reasonably extracted. This result calls attention to the need for careful documentation of surface drifter launch positions relative to the dynamic axis of the Gulf Stream so that resultant trajectories can be assessed in the context of their initial position. However, before these results can be used to interpret the likelihood that there was or was not a trend in the intergyre exchange measured by the North Atlantic

Table 2: Percent of drifters drogued to 15 m that reach 53°N when launched from various launch locations (rows) and advected through various horizontal velocity fields (columns).

	1991–1995 Forcing	1996-2000 Forcing	2001-2005 Forcing
1991-1995 Launch Locations	0.0 %	1.6%	0.8%
1996-2000 Launch Locations	0.5%	2.0%	1.6%
2001-2005 Launch Locations	2.3%	2.3%	0.4%

surface drifters, we must first assess whether drifters constrained to a depth of 15 m can reliably measure intergyre exchange.

The constraint imposed by the 2d motion of surface drifters on the measure of intergyre exchange is examined by repeating the test described above (with results shown in Table 2) using the full 3d velocity field for integration of the pathways rather than just the horizontal velocity field. For this run synthetic drifters, when allowed to move in 3d, become synthetic floats. As seen in Table 3, regardless of launch location or forcing, the number of synthetic floats reaching 53°N increases dramatically relative to the number of surface-constrained drifters reaching that latitude when launched under the same conditions. Whereas a maximum of 2.3% of surface drifters (at 15 m) reached 53°N, the percentage of floats reaching that latitude ranged from 6-29%, depending upon launch location and forcing. These results clearly indicate that BT's conjecture was likely correct: the inability of surface drifters to move in 3d inhibits their ability to mimic the

pathway of water parcels. Thus, these results suggest that in order to accurately measure intergyre exchange in the upper ocean, observational floats/drifters must be Lagrangian in nature and in the reconstruction of such pathways using model data, the 3d velocity field must be used. Additionally, these results highlight the bias introduced by variable launch locations in the assessment of temporal changes. Though intergyre exchange for a fixed launch location scheme varies across the HR pentads (by ~6-7% for all launch location schemes), the total variability in the percent of floats reaching 53°N is dominated by variability in launch location. Regardless of the velocity field through which floats were advected, floats launched from the 1991-1995 and 2001-2005 pentads measured a maximum of 14.0% exchange. However, floats launched from the 1996-2000 locations and advected through the velocity fields from each of the HR pentads measured from 21.7 to 29.1% exchange. As described previously, launches from the second HR pentad contain a number of launch locations north of the GS front (Figure 13a). As such, the amount of exchange measured by the 3d floats shown in Table 3 for this pentad is likely an overestimate.

In answer to the question posed at the beginning of this section, we conclude that the results from the synthetic drifter launches in FLAME indicate that intergyre exchange measured by observed drifters is likely constrained by limited drifter lifetimes, but even more likely limited by the inability of the drifters to move away from the 15 m surface. Furthermore, the modeling experiments suggest that variability in launch location

Table 3: Percent of floats launched at 15 m that reach 53°N when launched from various launch locations (rows) and advected in 3d through various velocity fields (columns).

	1991-1995 Forcing	1996-2000 Forcing	2001-2005 Forcing
1991-1995 Launch Locations	10.1 %	6.1%	12.2%
1996-2000 Launch Locations	21.7%	28.0%	29.1%
2001-2005 Launch Locations	7.4%	10.1%	14.0%

prohibits an assessment of temporal variability in subtropical to subpolar pathways from the observational record.

3.4.1.2 Could the removal of Ekman velocities allow for a meaningful measure of exchange by surface drifters?

Based on BT's conjecture that Ekman transport inhibits surface exchange, we investigate in this section the possibility that the removal of the Ekman velocity field (calculated from the observed wind field) could yield an estimate of throughput from the observed drifters. The depth of the fair weather Ekman layer in stratified, mid-latitude regions of the North Atlantic has been estimated to be 20 m or less [*Price and Sundermeyer, 1999*]. As such, the tests conducted in Section 3.4.1.1 are duplicated in this section for synthetic drifters launched at 50 m, sufficiently deep to be below the depth of the mid-latitude Ekman layer and advected through the 2d velocity fields. Essentially, with this modeling experiment we ask whether, given the other observational constraints of limited drifter

lifetime and variable launch locations, an accurate measure of the intergyre exchange and its temporal variability can be retrieved with the removal of the Ekman velocity field.

Despite the results from the previous section that showed the importance of integrating the surface drifters with the 3d velocity field, we conduct these experiments using the 2d velocity field in order to assess the degree to which useful information about intergyre exchange can be extracted from the observational dataset. With this choice, we are assessing whether the observational database is sufficient to recover the subsurface (50 m) pathways from the subtropical to the subpolar gyre.

The effect of drifter lifetime is first retested by launching synthetic drifters at 50 m from the launch locations of each HR pentad and integrating forward in time for four years.

The results, shown in Figure 15, clearly indicate that the amount of exchange below the Ekman layer exceeds that at the surface: whereas 17% of drifters with lifetimes of 4 years enter the subpolar gyre at 50 m (Figure 15c), none of the drifters launched from the same launch locations and advected through the same velocity fields reach the subpolar gyre when launched at 15 m (Figure 14a). Furthermore, drifter lifetime appears to play a much more substantial role in the amount of measured exchange at 50 m than it did at the surface. As shown in Figure 15, only 2% of drifters with lifetimes of 270 days (the mean lifetime of drifters in the observational record) enter the subpolar gyre when launched at 50 m, while (7%) 17% of drifters with lifetimes of (600 days) 4 years do so. This dramatic increase in exchange with drifter lifetime at 50 m clearly indicates that drifter lifetimes of 270 days are insufficient to capture intergyre pathways below the Ekman

layer. Furthermore, this trend was found to be consistent for drifters launched in all HR pentads and from all locations (not shown).

Given the insufficiency of the observed drifter lifetimes to measure intergyre exchange and its temporal variability, we next ask whether a measure of exchange could be recovered from the observed data set if the observed drifter lifetime was extended via BT's "linkage" method described in Section 3.2. Toward this end, the 9-part modeling experiment described in Section 3.4.1.1 (with results shown in Table 2) is repeated for drifters launched below the Ekman layer (at 50 m) and allowed to run for 4 years. Again, nine runs are made, whereby pathways are initiated from each of the observational launch schemes and integrated forward with the velocity fields from each of the three pentads. An inspection of Figure 16 demonstrates that, as with drifters launched within the Ekman layer, the effect of launch location proves to be much more influential in establishing the number of drifters reaching the subpolar gyre than temporal variability in the velocity fields through which they are advected. For example, the amount of exchange measured for drifters launched from the 1991-1995 observational launch locations and advected through the velocity fields from each of the HR pentads measures 17%, 14% and 11% respectively (top row, Figure 16). In contrast, the amount of exchange measured by drifters launched from each of the three sets of observational launch locations and advected through the 1991-1995 velocity fields yields a 17%, 54% and 16% rate of exchange (left column, Figure 16). Once again, drifters launched from the launch locations of the second HR pentad (1996-2000) yield the greatest rate of exchange.

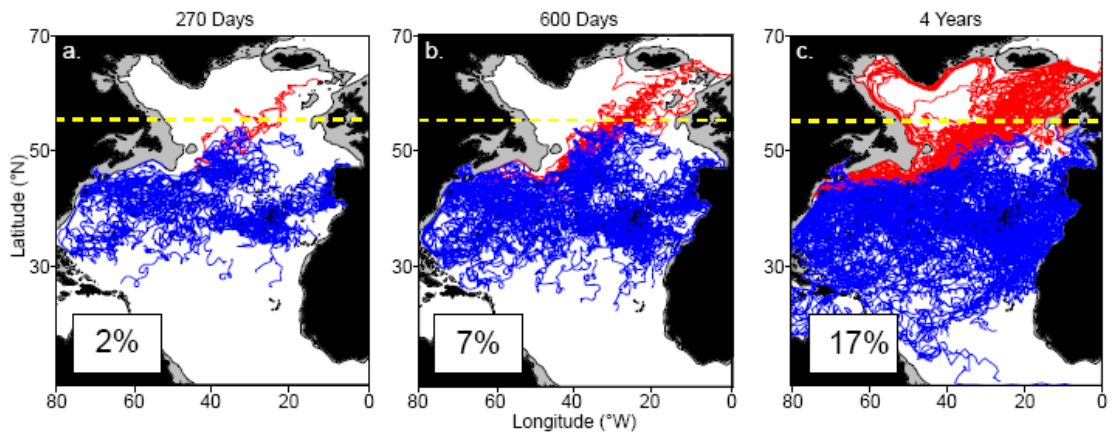


Figure 15: Synthetic drifters released below the Ekman layer (50 m) from the observational launch locations (Figure 13a) for the first HR pentad (1991-1995) and advected through the instantaneous horizontal velocity fields for (a) 270 days (average lifetime of the drifters in the observational record) (b) 600 days (long lifetime run used in BT study) and (c) 4 years. Colors are as in Figure 14. Bathymetry less than 500 m is shaded gray.

In summary, these modeling experiments suggest that the irregularity and variability of the initial launch locations as well as the inability of the floats to move in 3d space pose large obstacles to obtaining a realistic assessment of the observed Lagrangian intergyre exchange and its temporal variability from the observational dataset. Even if the effect of limited drifter lifetime can be alleviated and the Ekman velocity field removed, the observational drifter data set is sufficiently hampered by these constraints to preclude reliable estimates of exchange. With this conclusion and that from the previous section regarding the importance of 3d pathways, we can no longer look to the current observational database for a depiction of intergyre exchange from a Lagrangian viewpoint. As such, we continue our study within the context of FLAME using synthetic floats advected with the 3d velocity field and launched from a regular grid within subtropical waters. We do not suppose that the model will yield the North Atlantic's subtropical to subpolar exchange, rather that a comparison of the model's subsurface to surface exchange will provide context for the rather sparse observational dataset.

3.4.2 Is the amount of intergyre exchange at the surface representative of the overall subtropical to subpolar exchange?

In order to investigate the nature of subtropical to subpolar exchange within FLAME, synthetic floats were launched dynamically within the Gulf Stream grid (described in Section 3.3) and integrated forward in time for 4 years using the time-varying 3d velocity field. Floats were repeatedly launched every 2 months between 1990 and 2000 (launches

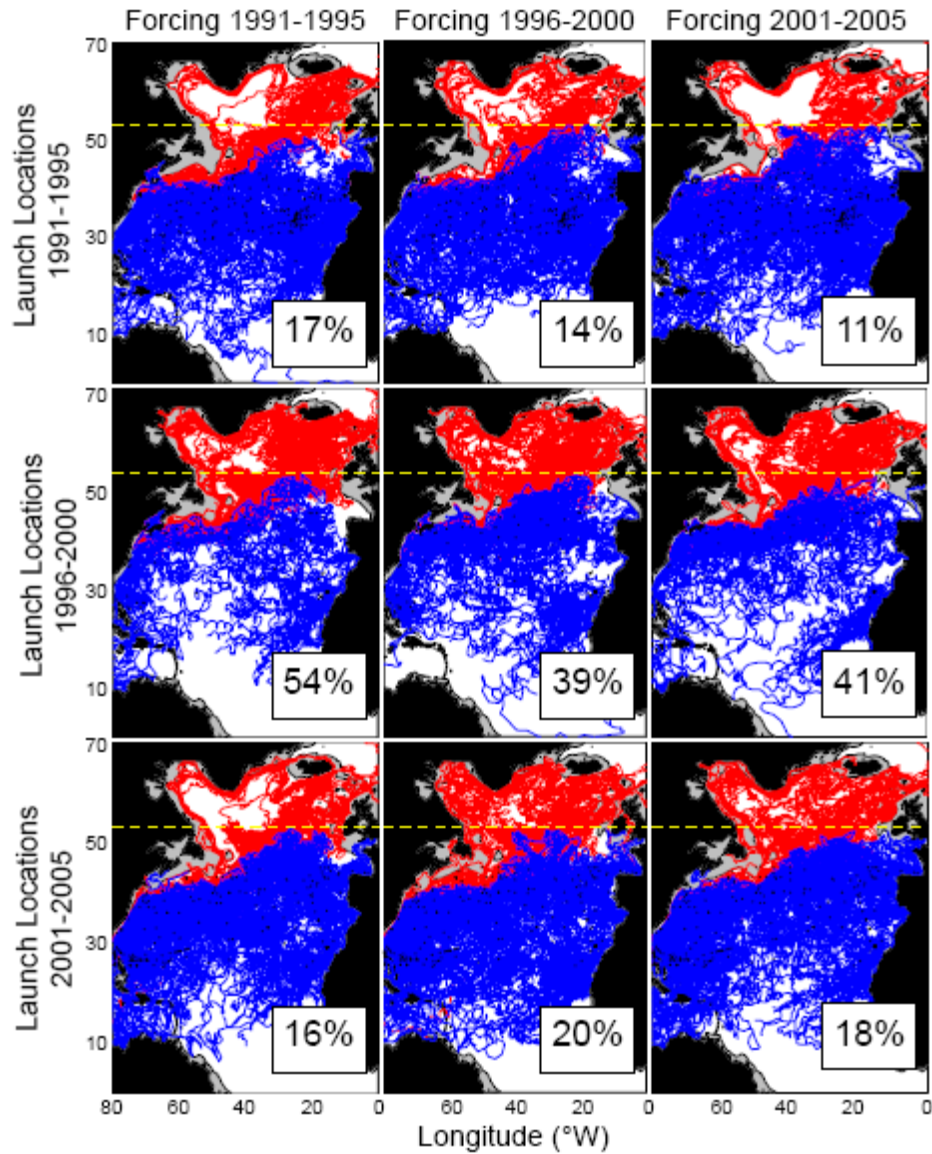


Figure 16: Relationship between launch positions and pentad of the modeled circulation in the delivery of 50 m drifters to the subpolar domain. Synthetic drifters launched in FLAME at the observational launch locations (Figure 13a) for each of the three HR pentads (row 1) 1991-1995, (row 2) 1996-2000 and (row 3) 2001-2005 and advected through the instantaneous 50 m horizontal velocity fields from (column 1) 1991-1995, (column 2) 1996-2000 and (column 3) 2001-2005 for 4 years. Colors are as in Figure 14. Bathymetry less than 500 m is shaded gray.

after 2000 would not yield 4-year trajectories). As described previously, care was taken to ensure that only floats whose initial position lay south of the instantaneous Gulf after 2000 would not yield 4-year trajectories). As described previously, care was taken to ensure that only floats whose initial position lay south of the instantaneous Gulf Stream front were considered. Finally, floats were launched at 15 m, 50 m and also at 100 m intervals between 100-1300 m in order to assess the vertical profile of intergyre exchange for the upper water column.

The model runs described above produce the vertical profile of Lagrangian intergyre exchange shown in Figure 17, where error bars are derived from repeated launches. A sample of the resultant trajectories from these launches can be seen plotted according to launch depth in Figure 18a. As evident in Figures 17 and 18a, the exchange measured by the floats launched at 15 m, whose northward transport is inhibited both by their launch positions south of the Gulf Stream front and, at least initially, by Ekman drift is small: only $3 \pm 1\%$ of floats reach 53°N within 4 years. However, below the Ekman layer the number of floats reaching the subpolar gyre increases steadily until reaching a subsurface maximum of 30% ($\pm 3\%$) for floats launched at 700m.

Spall [1992] demonstrated that cooling of subtropical surface waters in a non-eddy-resolving model with steady forcing can produce velocities that spiral cyclonically with depth beneath the Gulf Stream's eastward extension. To examine whether the enhanced exchange with depth observed within FLAME, described in the preceding paragraph, can

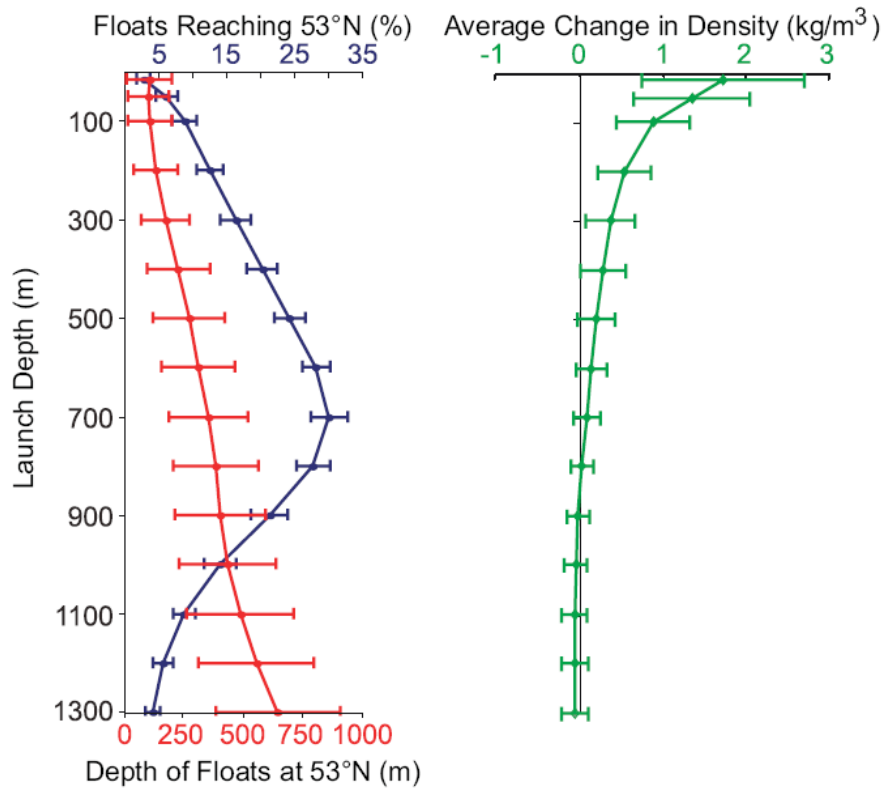


Figure 17: (left) (blue) Mean percent of synthetic floats launched at various depths which reach 53°N when advected through the 3d velocity field for four years. Error bars indicate the standard deviation of the percent of measured exchange recorded by floats from each of the launches initiated between 1990-2000. (red) Mean depth of all floats reaching 53°N when they arrive at 53°N. Error bars indicate the standard deviation of float depths when they arrive at 53°N. (right) (green) Average density change of all floats reaching 53°N between the time of their launch and the time that they cross 53°N. Error bars indicate the standard deviation of float density change.

be explained by such a cooling spiral, the vertical structure of the mean velocity field in FLAME was examined at several locations along a launch transect at 48°W (Figure 18a). Shown in Figure 18b is the mean velocity hodograph along that transect at 38°N, which is just south of the climatological position of the Gulf Stream front (Figure 13a) and within the region of strong wintertime cooling. A cyclonic rotation with depth of the upper water column (only velocities below the Ekman depth are plotted in Figure 18b since the cooling spiral pertains to the geostrophic velocities) is evident, however the rotation is weaker and shallower than that predicted by *Spall* [1992] for the subtropical gyre. The spiral shown in Figure 18b has a rotation of just 5.35° from 50 to 200m, compared to a predicted rotation of 27° over 450 m. Below 200 m an anticyclonic beta spiral [*Schott and Stommel*, 1978] is recovered. Inspections of hodographs at other locations along the transect produced similar results. Interestingly, the spiral in the model's winter velocity field is weaker (~1° from 100 to 300m) than that shown in Figure 18b, lending some doubt to the supposition that the cooling is responsible for the observed spiral and, consequently, differences in exchange with depth. Furthermore, if the escape of the floats considered in Figure 17 was primarily determined by the presence of a wintertime cooling spiral, some seasonality in the arrival into the subpolar gyre would be expected. However, an examination of the arrival time of floats in the subpolar gyre (not shown) indicated none of the expected seasonal variability and, perhaps more relevant, there was no preference when the floats that arrived at 53°N were sorted by the season of their launch. Finally, we note that the increase in float exchange with depth extends to 700 m, at which point the exchange is maximized. Thus, it is difficult to

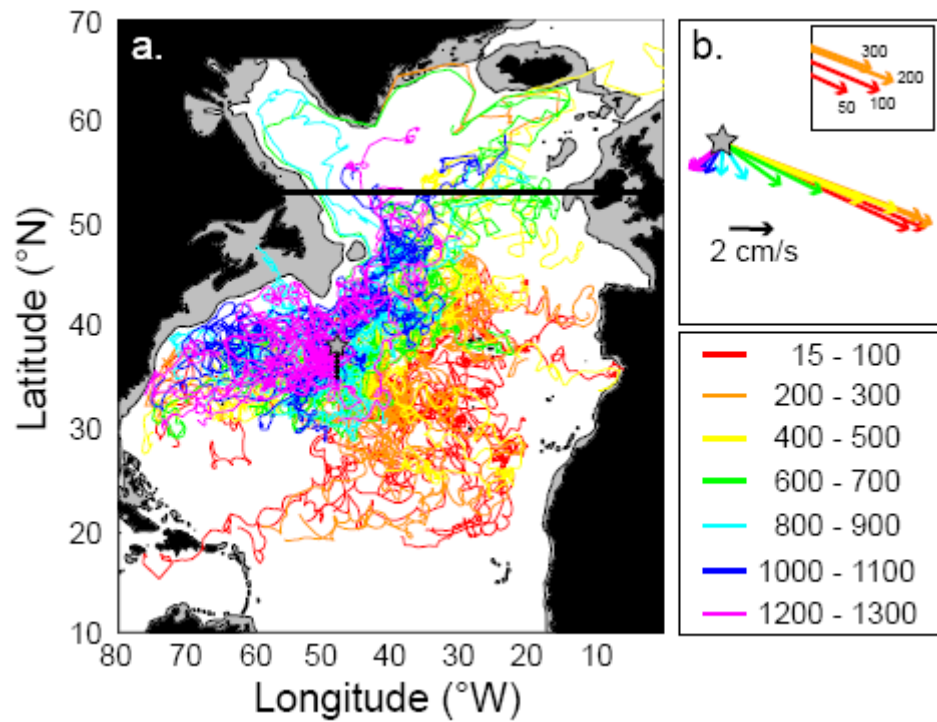


Figure 18: Changes in velocities and synthetic float trajectories with depth in FLAME. (a) Trajectories of synthetic floats launched along a transect at 48°W within the Gulf Stream grid and advected through the instantaneous 3d velocity fields for 4 years. Colors indicate the depth of the float at the time of its launch. Bathymetry less than 500 m is shaded gray. Gray star indicates the location of the mean velocity profiles shown in (b). (b) Mean velocities from 50-1300 m at 48°W, 38°N.

attribute exchange characteristics within the model to a weak cooling spiral that extends to only 200 m in the mean and one that is not consistent with seasonal expectations. The depths at which floats within the Gulf Stream grid arrive at 53°N (henceforth, the “target depth” of the floats) are indicated by the red line in Figure 17. An examination of float target depths indicates that, with the exception of floats launched at 15, 50 and 100 m (which each have average target depths of ~100 m), the floats shoal significantly as they move northward, often arriving hundreds of meters shallower than their launch depth. For example, the average target depth of floats launched at 700 m is 350 (± 166) m. This shoaling of float positions is supported by the mean position of isopycnals along 40°W between 25 and 60°N (Figure 19), where strong shoaling of the isopycnals across the subtropical/subpolar front is evident. Interestingly, the shallowest density surfaces along 40°W are restricted to low latitudes, outcropping at the surface south of the mean position of the NAC (depicted by the strong vertical gray lines in Figure 19) suggesting that surface waters within the subtropical gyre are largely recirculated. However, the isopycnals found at depth in the subtropical gyre, including the $\sigma_{\theta} = 27.1$ surface (shown by the strong white line in Figure 19) cross the NAC as they shoal and outcrop north of the front.

From Figure 17 it appears that floats arrive at 53°N at the depth which their launch isopycnal resides. In other words, it appears as though the change in depth of the floats from their launch location to 53°N can be attributed to the shoaling of the isopycnals from the subtropical to the subpolar gyre. However, the target depths of the floats at

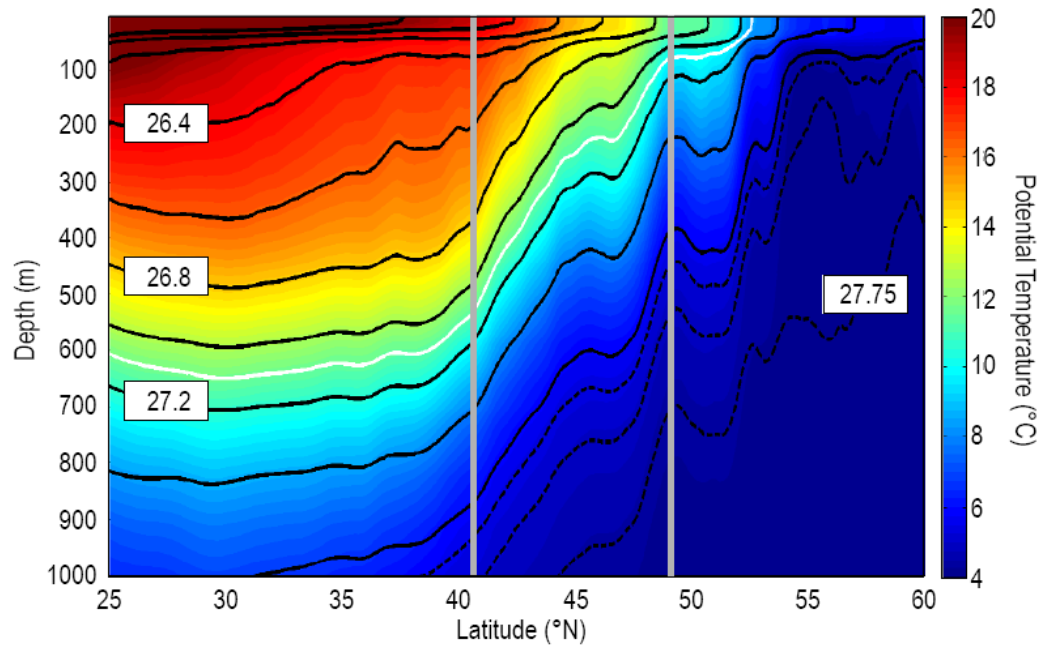


Figure 19: Isopycnal structure along 40°W in FLAME. Mean potential density superposed over mean potential temperature along a meridional section at 40°W in FLAME. Contour interval is 0.2 kg/m³ and 0.05 kg/m³ for solid and dashed black lines respectively. White contour indicates the $\sigma_{\theta} = 27.1$ isopycnal. Gray bars indicate the mean position of the NAC at 40°W.

53°N are slightly deeper than the depth of the launch isopycnals, indicating that some densification occurs along float pathways (Figure 17). This densification likely results from cooling due to the strong loss of heat to the atmosphere along the pathway of the NAC [McCartney and Talley, 1982] and mixing with denser water masses as the floats make their way to the north. While the surface water densification is substantial (more than the density change across the front at their launch location; see Figure 19), it is important to note that the floats launched at deeper levels, which comprise the bulk of the floats reaching the subpolar gyre, remain close to their original densities. For example, floats launched at 700 m experience only $\sim 0.1 \text{ kg/m}^3$ densification between their launch locations and 53°N (Figure 17), which is about 1/5 of the cross-stream density gradient at their launch location (Figure 19). Thus, though some densification does occur along pathways, these modeling experiments suggest that subtropical waters entering the subpolar gyre are primarily subsurface waters that shoal along density surfaces as they move northward.

To complement the cross-section of temperature and density in Figure 19, plan views of depth and potential vorticity on two selected isopycnals are shown in Figure 20. As emphasized above, the depth contours on the shallow isopycnal (Figure 20a) indicate that waters this light are absent north of $\sim 45^\circ\text{N}$ [Lozier *et. al*, 1995]. Instead these relatively shallow waters recirculate within the subtropical gyre, as indicated above by float pathways, but also indicated by the potential vorticity field in this basin. Prior modeling work has demonstrated the constraint placed on Lagrangian pathways by the mean

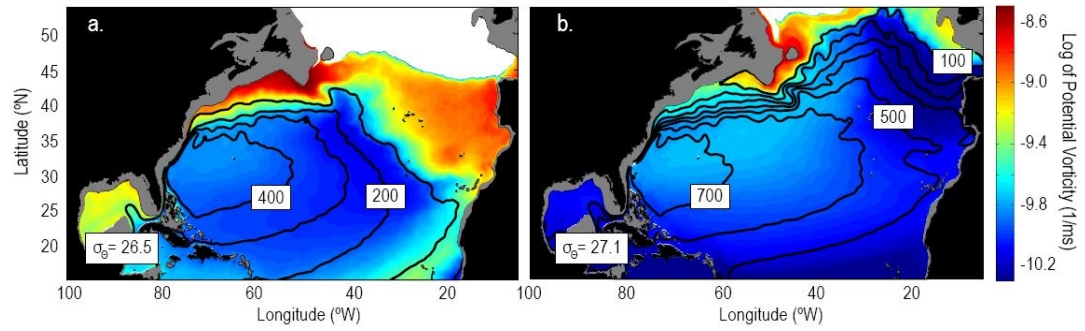


Figure 20: Mean depth (m) of the (a) $\sigma_\theta = 26.5$ and (b) $\sigma_\theta = 27.1$ isopycnal surfaces superposed on mean potential vorticity fields along those isopycnals in FLAME. Depth contour interval is 100 m. Bathymetry below 500 m is shaded gray.

potential vorticity in a subtropical basin [Lozier and Riser, 1990]. For the deeper isopycnal, at the approximate depth where Lagrangian pathways are most likely to lead from the subtropical launch region to the subpolar latitudes, the potential vorticity field is consistent with a bifurcation at the exit of the Gulf Stream. Such a bifurcation (long noted in past studies of hydrographic fields) suggests a flow field that contains a branch that recirculates anticyclonically in the subtropical basin and another that extends to subpolar latitudes; consistent with the Lagrangian pathways. This extension is, in effect, the throughput of subtropical waters as part of the basin scale meridional overturning.

3.5 Summary

For decades the Gulf Stream/North Atlantic Current system has been considered the dominant pathway by which subtropical waters are advected to high latitudes. The visual connectivity between the subtropical and subpolar gyres, apparent in surface velocity and sea surface temperature fields, has led to the supposition of a strong surface throughput. As such, previous studies have used surface drifter records in an attempt to understand both the mean and time-varying pathways by which subtropical waters are transported to the subpolar gyre.

In this study, an eddy-resolving OGCM was used to demonstrate that drifters from the observational record are more than likely incapable of capturing the true pathways by which subtropical waters are transported to high latitude regions of deep convection as a

result of their short lifetimes (as demonstrated previously by BT), variable launch locations and restriction to movement in 2d. Synthetic floats were repeatedly launched from a standard grid and integrated for four years with the model's 3d velocity field to study intergyre exchange. From the modeling results, we suggest that subtropical waters in the North Atlantic are primarily transported to high latitudes at depth along shoaling density surfaces. Surface waters in the subtropical gyre, sampled by the drifters in the observational record, are largely absent in the intergyre exchange process and are instead recirculated within the subtropical gyre.

Recent evidence regarding the impact of wind and eddy fields on the circulation of the North Atlantic has revealed that the "conveyor belt" model greatly oversimplifies the large scale overturning of the ocean [*Lozier*, 2010 and references therein]. This study reinforces the complexity of the overturning since it calls into question the expectation that the conveyor belt has a strong surface expression in the intergyre transport in the North Atlantic. The implication of this result for our understanding of how overturning variability impacts the spatial and temporal variability of the North Atlantic's sea surface temperature remains unanswered.

4. Understanding the Oceanic Transport of Heat to the Eastern Subpolar Gyre

4.1 Introduction and Background

Sea surface temperature (SST) has long been recognized as an important factor in establishing global temperature and precipitation patterns. In the North Atlantic, the relatively warm SSTs of the eastern subpolar gyre ($>10^{\circ}\text{C}$ above the zonal average, Figure 21) have been widely linked to the moderate winter temperatures of Great Britain and western Europe as well as to the high rates of precipitation experienced in those regions. Historically, the zonal asymmetry in subpolar sea surface temperatures has been assumed to be the result of warm surface waters transported from the western subtropical gyre to the eastern subpolar gyre (ESG) by a strong and continuous Gulf Stream (GS) and North Atlantic Current (NAC) system. This transport is believed to be the upper limb of the meridional overturning circulation, in which the GS/NAC system transports warm surface waters directly from low to high latitudes in order to replenish the surface waters in the regions of deep convection. However, recent examinations of Lagrangian floats and drifters have suggested that this surface pathway may play only a minor role in transporting heat to this climatically important region.

In their study of synthetic floats in a high resolution ocean general circulation model (OGCM), *Burkholder and Lozier* [2011] (henceforth BL) examined the Lagrangian pathways of floats released at various depths in the Gulf Stream region of the subtropical gyre in order to examine Lagrangian transport pathways connecting the Gulf Stream region to high latitudes. The results of their study demonstrated that only a small fraction (<5%) of floats released in the surface waters of the Gulf Stream region were able to successfully reach high latitudes within 4 years, highlighting a lack of continuity between the surface waters of the subtropical and subpolar gyres. Importantly, this lack of surface water connectivity has also appeared in the observational record: a study [*Brambilla and Talley*, 2006, henceforth BT] that analyzed the trajectories of 273 surface drifters passing through the Gulf Stream region between 1990-2002 noted that only 1 drifter was able to reach the subpolar gyre within its lifetime. Taken together, the modeled and observed results strongly suggest that the traditional understanding of surface water throughput from the subtropics to the ESG via the GS/NAC system is not supportable. Thus, the pathways that supply the surface waters of the ESG remain unclear.

Although the focus of both the BL and BT studies was on the export of waters from the Gulf Stream region, these studies offer clues as to potential Lagrangian pathways that lead to the ESG surface waters. In BL, which examined synthetic floats launched in the Gulf Stream region throughout the upper water column (15-1300 m), the ability of floats to reach high latitudes appeared to be maximized subsurface; though the number of surface-launched drifters able to reach the subpolar gyre was minimal (<5%),

approximately 30% of floats launched at 700 m (mean density $\sigma_\theta = 27.27$) in the Gulf Stream region reached high latitudes. These floats, which shoaled significantly along isopycnal surfaces as they progressed northward, eventually entered subpolar latitudes (53°N in BL) at ~350m, well below the depth of the average winter mixed layer in the region. Although the influence of these deeper trajectories on the surface waters of the subpolar gyre has remained unclear to date, the results from the BL study indicate that subsurface pathways may play an important role in supplying the ESG.

The BT study of surface drifters also suggested an alternative pathway by which waters may reach the ESG. After examining the trajectories of the many drifters that entered the Icelandic basin between 1990-2002, BT determined that only 1 of the drifters originated south of 45°N (their Figure 4b). As with the subtropical drifters analyzed in their study, the subpolar surface drifters were shown to largely recirculate within their gyre of origin for the duration of their lifetime. BT were careful to acknowledge that the drifters analyzed in their study were very likely limited in their ability to track true Lagrangian pathways as a result of their inability to move in three dimensions. Nevertheless, in the present study, recirculated subpolar surface waters are investigated as a possible source of waters to the ESG.

The main goals of the present study are to identify the Lagrangian pathways that supply the climactically important surface waters of the ESG and to characterize the roles of the pathways in supplying heat to the region of warm SSTs. By addressing these issues, we

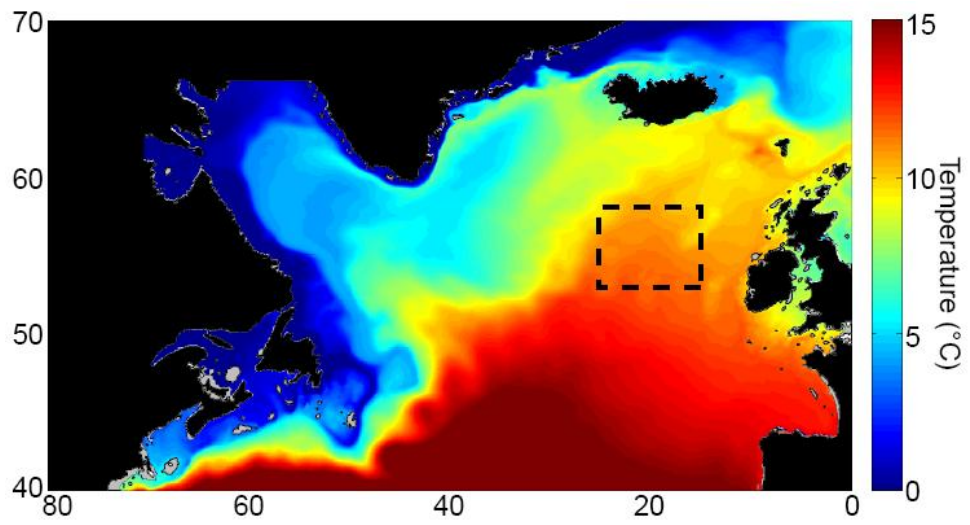


Figure 21: Climatologically averaged temperatures at 50 m in FLAME. Black box indicates the box surrounding the launch positions of ESG floats. Bathymetry ≤ 50 m is shown in gray.

aim to provide a better understanding of the controls on high latitude sea surface temperatures in a region where the impacts of changes to those temperatures have been well documented. A description of the methods and the high resolution model used in this study is given in Section 4.2, followed by a discussion of the study results in Section 4.3. Finally, a summary is provided in Section 4.4.

4.2 Methods

In order to identify and characterize pathways leading to the ESG, this study utilizes 15 years of output from a realization of the 1/12° resolution FLAME OGCM (**F**amily of **L**inked **A**tlantic **M**odel **E**xperiments) [Böning *et al.*, 2006; Biastoch *et al.*, 2008].

FLAME was previously described in Chapters 2 and 3 of this dissertation. In the present study, FLAME velocity fields were used to produce synthetic “reverse trajectories” in which floats were launched in the ESG then advected backwards in time through the full 3d velocity fields in order to determine their region of origin. Floats were seeded at 1/2° x 1/2° intervals within a launch box stretching from 25-15°W and 53-58°N (black box, Figure 21). For consistency with the BL study, which investigated subtropical to subpolar gyre exchange, floats were released in monthly batches and run with lifetimes of 4 years.

In order to fully examine the influences of various pathways on the subpolar gyre, launches were conducted from a variety of depths. During each initialization of floats in

the subpolar gyre, sets of floats were launched at 5 m, 50 m, 100 m and 350 m. These locations were chosen in order to highlight the contribution of Lagrangian pathways to subpolar waters that are located at the sea surface (5 m), at the base of the Ekman layer (50 m), below the Ekman layer (100 m) and below the direct influence of the atmosphere (350 m). The 350 m floats also coincided with the average “target depth” of the 700 m floats from the BL study (the floats that were the most successful at reaching the subpolar gyre). 100 randomly selected trajectories from the launches at each of these depths are plotted in Figure 22.

The trajectories shown in Figure 22 are separated into three groups: (1, red) those that originated in the western subtropical gyre (henceforth called subtropical floats), (2, blue) those that originated in the western subpolar gyre (henceforth called subpolar floats, and (3, yellow) those that had no clear launch origin (henceforth called other floats).

Subtropical floats were considered to be all floats that reached latitudes south of 32°N during their lifetime, a definition chosen to ensure that subpolar floats caught in the recirculation gyre north of the Gulf Stream front [Hogg *et al.*, 1986] were excluded.

Subpolar floats were those that originated north of 60°N and west of 45°W. Other floats were those floats that did not cross the subtropical or subpolar boundary during their lifetime. With these delineations, >80% of the floats were accounted for when launched from 5, 50 and 100 m. Though only 49% of the floats launched at 350 m were captured when run with lifetimes of 4 years, a test of floats with 10-year lifetimes confirmed that these small percentages likely result from the slower velocities of floats at 350 m. When

run for 10 years, ~84% of 350 m floats were separated into the subpolar and subtropical pathways. However, in order to maintain consistency with the BL study, the 350 m results presented in Section 4.3, unless otherwise noted, come from the set of floats with 4-year lifetimes.

4.3 Results

4.3.1 Determination of Lagrangian Pathways Supplying the ESG

As evident in the trajectories shown in Figure 22, regardless of launch depth, the vast majority of floats reaching the ESG originated in the subtropics, with $\geq 75\%$ of floats launched at 5, 50 and 100 m following the subtropical pathway (Table 4). Though only 45% of floats launched at 350 m originated below 32°N , the supplementary launch of drifters at 350 m indicated that 76% of 10-year floats originated in the subtropical gyre. In contrast, this analysis of float origin indicates that $<15\%$ of floats reaching the launch box were carried to the ESG by the subpolar pathway, regardless of the depth at which the floats were launched.

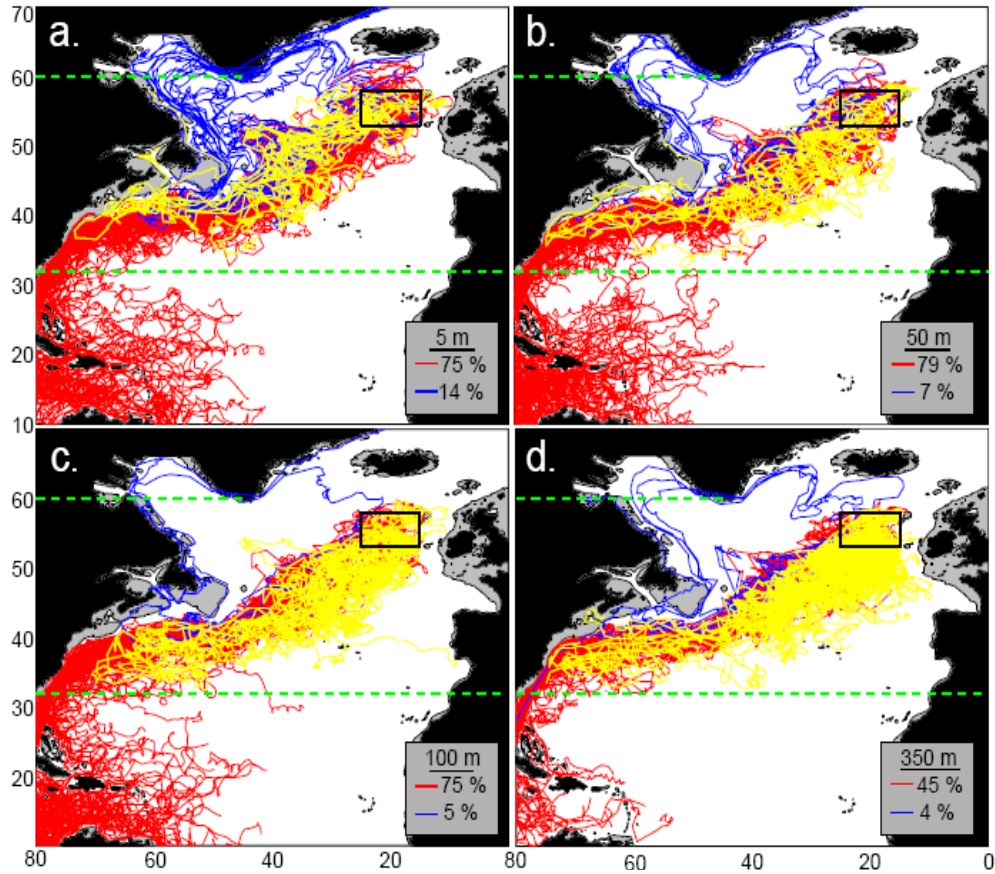


Figure 22: Trajectories of 100 randomly selected floats advected backwards in time for 4 years from the ESG (black box) when launched at (a) 5 m (b) 50 m (c) 100 m and (d) 350 m. Floats arriving from the subtropical and subpolar pathways are shown in red and blue respectively. Yellow trajectories indicate those floats that did not originate in either the subtropical or subpolar regions (other floats). Mean percentages of floats arriving from each pathway are shown in the gray box. Green lines indicate the 32°N and 60°N boundaries used to qualify floats as following the subtropical and subpolar pathways respectively. Bathymetry ≤ 200 m is shown in gray.

Table 4: Number of floats (%) launched at various depths within the ESG that reached the ESG via the subtropical (left) and subpolar (right) pathways described in Section 4.3.1 and shown in Figure 22. Errors indicate the standard deviation of the percentage of floats arriving from each pathway.

Depth in Subpolar Gyre (m)	% Subtropical Pathway	% Subpolar Pathway
5	75 ± 6	14 ± 6
50	79 ± 4	7 ± 2
100	75 ± 4	5 ± 2
350	45 ± 5	4 ± 1

The relatively small fraction of floats originating in the western subpolar gyre provides new insight into the interpretation of the high latitude Lagrangian drifters analyzed by BT (as described in Section 4.1), which indicated that almost 100% of floats entering the ESG originated in the western portion of the gyre. The absence of a large degree of recirculation of the synthetic floats, which have the ability to move in 3d, validates BT's conjecture about the drifters analyzed in their study: the inability of subpolar surface drifters to move in 3d inhibits their ability to follow true Lagrangian pathways. The evolution of density, temperature and depth along the pathways that lead to the ESG are examined next.

4.3.1.1 The Subpolar Pathway

As described in the previous section, a relatively small fraction of floats that enter the ESG have their origins in the western subpolar gyre. However, though the subpolar Lagrangian pathway does not appear dominant when compared with the subtropical

pathway, an analysis of changes in float properties along the subpolar path could offer insight into its role in transporting the (much colder) temperature signature of the western subpolar gyre across the basin. To that end, a population density map for the subpolar floats as they cross the 60°N boundary and exit the western subpolar gyre is provided in Figure 23. Interestingly, the distribution of the floats that exit the western subpolar gyre on their way to the eastern subpolar gyre indicates that the floats largely exit the subpolar gyre at the surface. The floats reaching 5, 50 and 100 m depths in the ESG had mean depths of 68, 65 and 72 m, respectively, when they crossed 60°N (henceforth “exit depths”, Table 5). The floats that reach the ESG at depths of 350 m have a mean exit depth of 127 m, although the spread around this mean is wide (± 106 m).

It is apparent in the 50 randomly selected subpolar trajectories analyzed in Figures 24-27 that regardless of launch depth (in the ESG), when floats exit the western subpolar gyre they move southward along the east coast of Canada as part of the Labrador Current. After rounding the Grand Banks, the floats intersect the subtropical pathways southeast of Newfoundland. Upon this intersection with the Gulf Stream/North Atlantic Current waters, the floats in general become deeper (Figure 24), warmer (Figure 25), saltier (Figure 26) and less dense (Figure 27). The exception to this generalization is the 5 m floats, which become warmer and less dense, but do not become noticeably deeper in this transition. This dramatic change in float properties indicates that strong mixing in the region of the Grand Banks, rather than transformation by the atmosphere is the likely cause of the change in float depth, temperature and density.

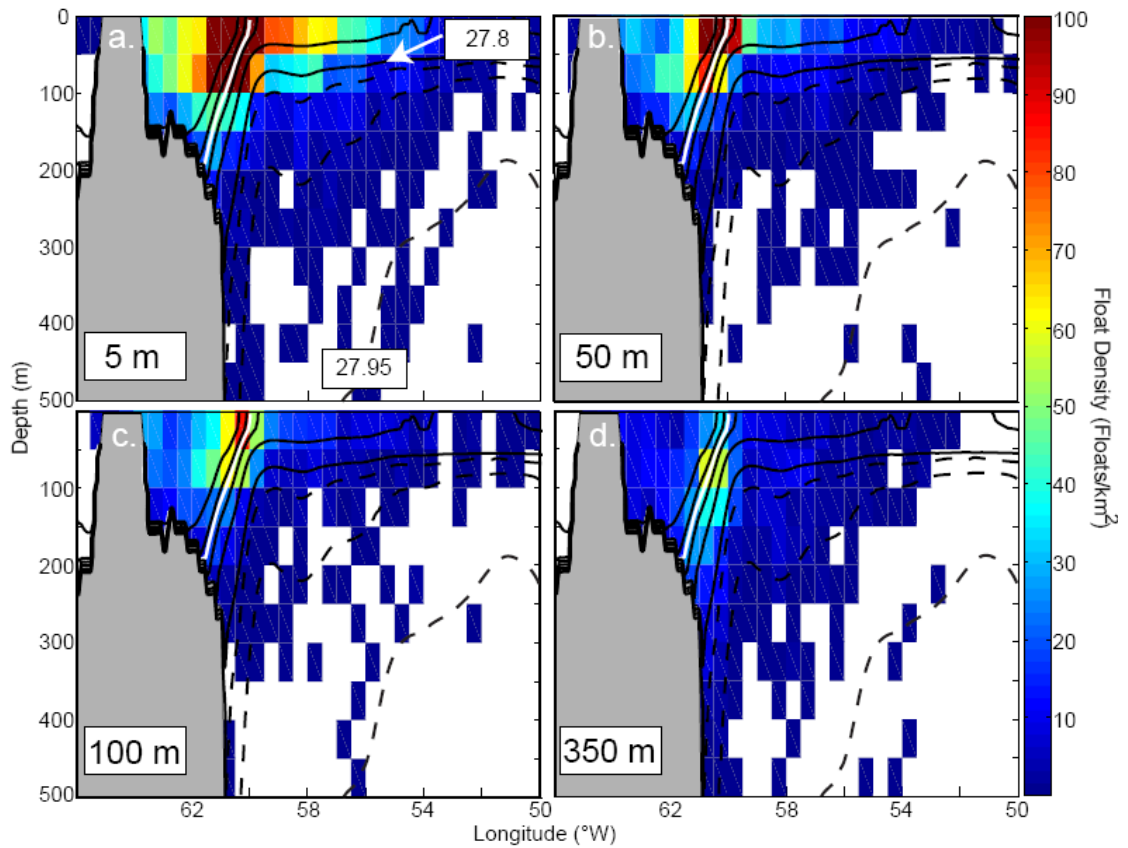


Figure 23: Density contours in the western subpolar gyre superposed over float density plots for those floats arriving at 60°N . Launch locations of the floats when initiated in the ESG are (a) 5 m (b) 50 m (c) 100 m and (d) 350 m. Bathymetry at 60°N is shown in gray. The contour interval is 0.2 kg/m^3 for the solid black lines and 0.05 kg/m^3 for the dashed lines. The climatological position of the $\sigma_{\theta} = 27.1$ isopycnal is shown in white.

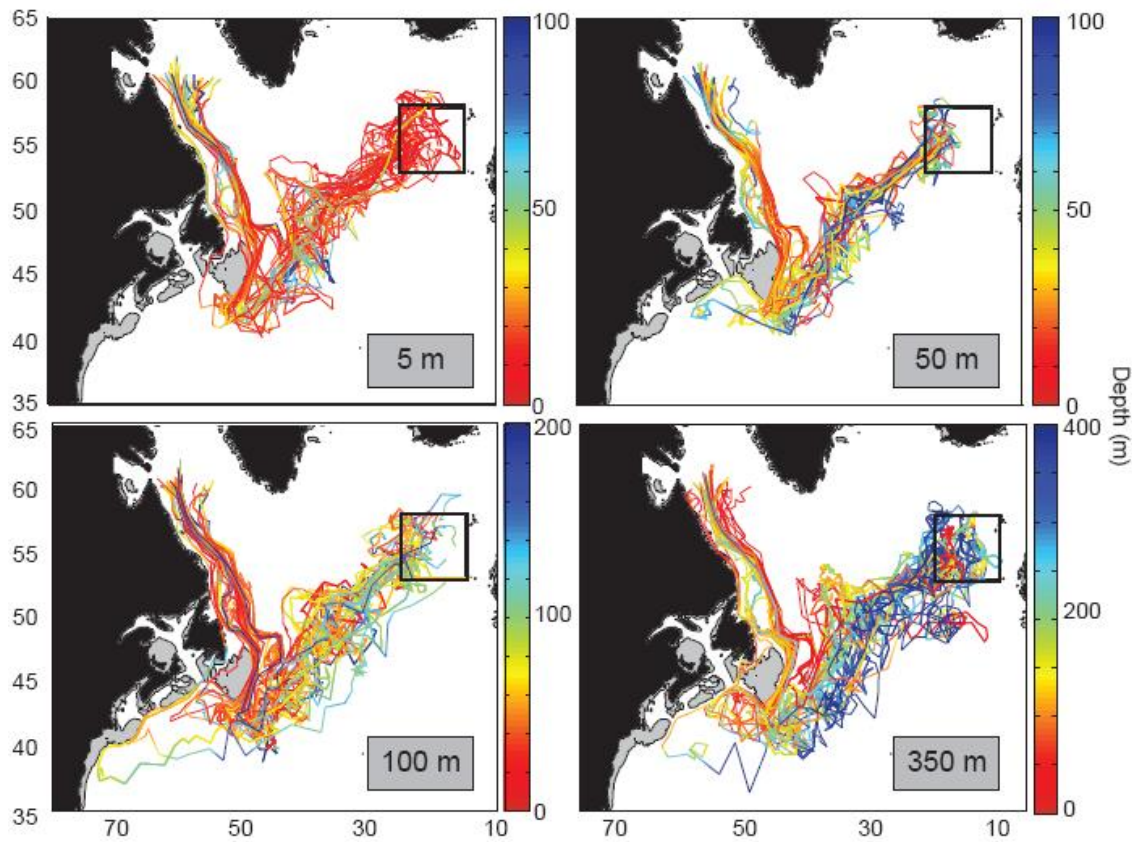


Figure 24: Depths of 50 randomly selected floats launched at (a) 5 m (b) 50 m (c) 100 m and (d) 350 m in the ESG as they are run backwards in time to their origin in the western subpolar gyre. Bathymetry ≤ 100 m is shown in gray.

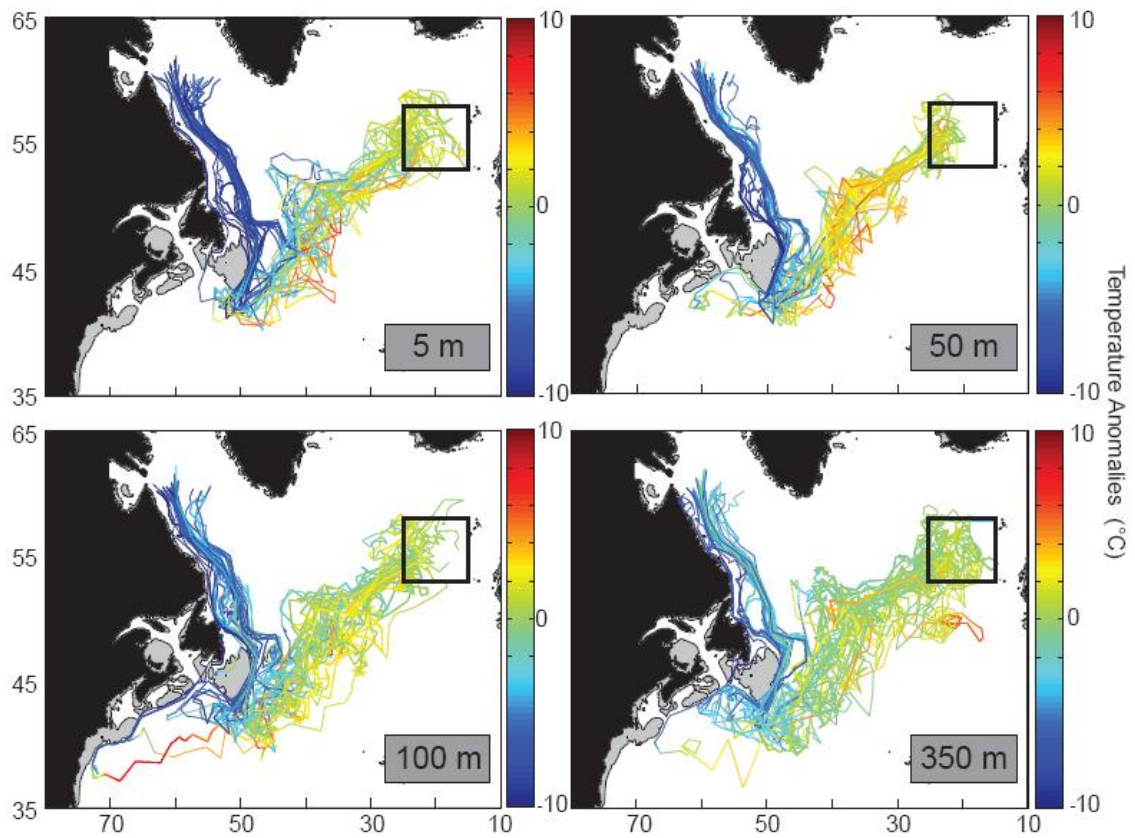


Figure 25: Temperature anomalies of 50 randomly selected floats launched at (a) 5 m (b) 50 m (c) 100 m and (d) 350 m in the ESG as they are run backwards in time to their origin in the western subpolar gyre. Colors indicate the difference in the temperature of the floats at a particular time and their temperature at the time of their launch in the ESG. Bathymetry ≤ 100 m is shown in gray.

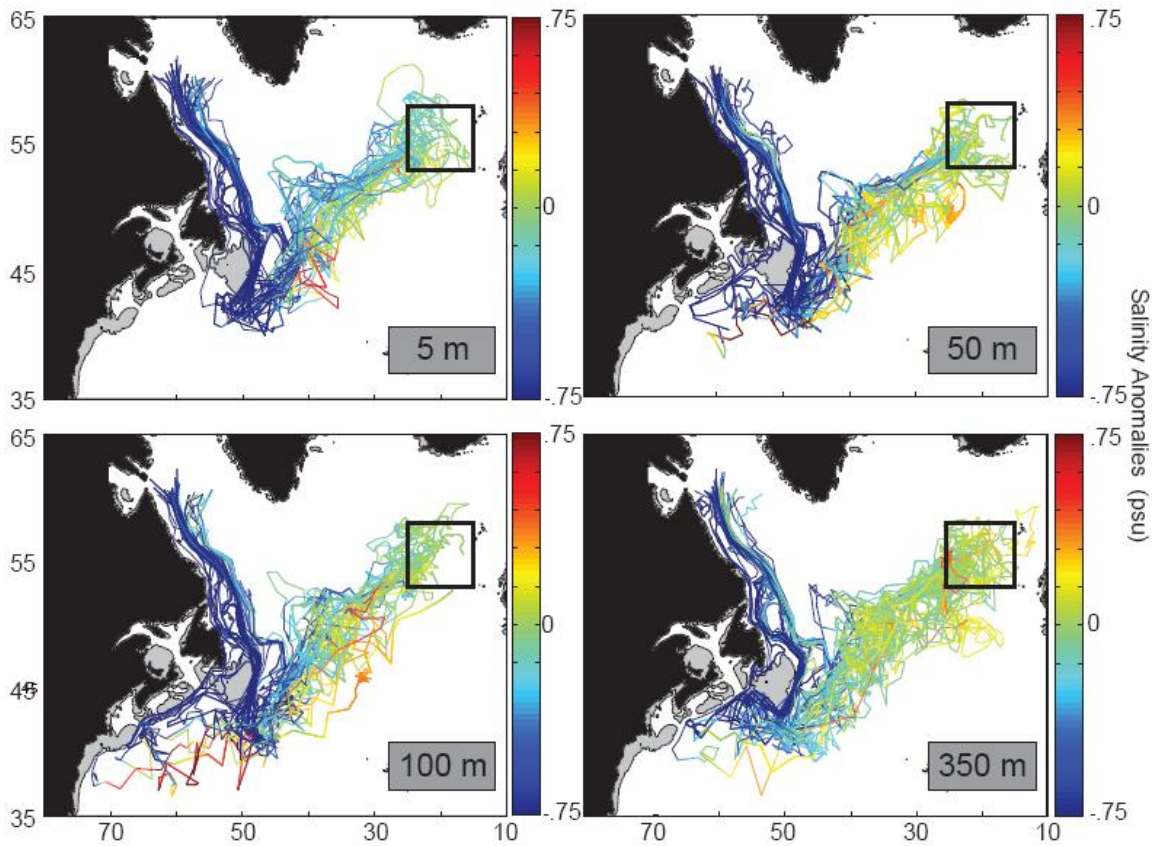


Figure 26: Salinity anomalies of 50 randomly selected floats launched at (a) 5 m (b) 50 m (c) 100 m and (d) 350 m in the ESG as they are run backwards in time to their origin in the western subpolar gyre. Colors indicate the difference in the temperature of the floats at a particular time and their temperature at the time of their launch in the ESG. Bathymetry ≤ 100 m is shown in gray.

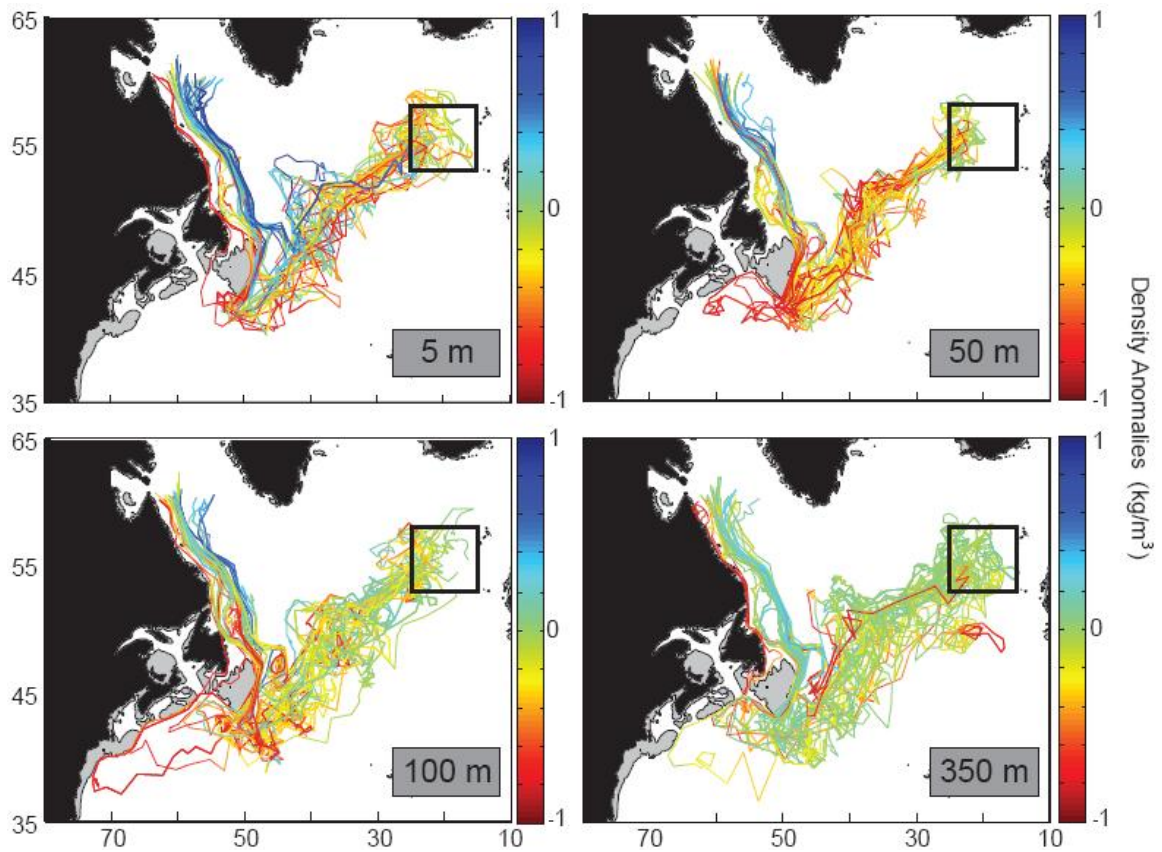


Figure 27: Density anomalies of 50 randomly selected floats launched at (a) 5 m (b) 50 m (c) 100 m and (d) 350 m in the ESG as they are run backwards in time to their origin in the western subpolar gyre. Colors indicate the difference in the density of the floats at a particular time and their density at the time of their launch in the ESG. Bathymetry ≤ 100 m is shown in gray.

Table 5: Mean depth of floats launched at various depths within the ESG when they cross the 32°N (subtropical) or 60°N (subpolar) boundary. Errors indicate the standard deviation of float depths.

Depth in Subpolar Gyre (m)	Depth at Subtropical Line (m)	Depth at Subpolar Line (m)
5	202 ± 143	68 ± 71
50	235 ± 153	65 ± 63
100	273 ± 167	72 ± 63
350	380 ± 214	127 ± 106

4.3.1.2 The Subtropical Pathway

Contrary to the results in Section 4.3.1.1, which indicate that the subpolar floats have their origins in the surface waters of the subpolar gyre, float population density maps at 32°N (Figure 28) indicate that regardless of launch depth, the exit depths of floats from the subtropical gyre are located below the surface (Table 5). Floats launched at 5, 50 and 100 m have mean depths of 202, 235 and 273 m, respectively, at 32°N. The deeper 350 m launches cross 32°N at a mean depth of 380 m, a location slightly shallower than may have been expected from the BL results, which indicated that the floats with the most success at reaching 53°N (which did so at a depth of 350 m) were those launched at 700 m in the subtropical gyre with average densities of 27.27 kg/m³. These differences will be discussed in detail in Section 4.3.2. As in the BL study, there is little evidence from the reverse floats launched in the ESG that surface waters are involved in the intergyre exchange process (Figure 28).

Predictably, as the subtropical floats are transported between the subtropical and subpolar gyres, they lose heat, arriving in the subpolar gyre with mean temperatures that are significantly cooler (Table 6, Figure 29) than when they exited the subtropical gyre. This change in temperature is accompanied by a freshening (Figure 30), a shoaling of float depth (Figure 31) and densification (Figure 32) along the subtropical pathway. However, unlike the property transition in the subpolar floats, the transition in float temperatures, densities and depths along the subtropical pathway appears to be gradual, with no particular location accounting for a significant loss of heat along the path. Instead, the property changes recorded by the subtropical floats likely result from the mixing of subtropical waters with denser waters along the path of the Gulf Stream and North Atlantic Current and, in the case of the shallower waters, loss of heat to the atmosphere [McCartney and Talley, 1982]. However, though some of the heat from the subtropical waters is likely lost to the atmosphere, the subsurface subtropical pathway appears to be the dominant oceanic source of heat to the ESG.

Table 6: Mean change in temperature of floats as they progress along the subtropical (left) and subpolar (right) pathway to the ESG box. Errors indicate the standard deviation of float temperature change.

Depth in Subpolar Gyre (m)	Temperature Change along Subtropical Path (°C)	Temperature Change along Subpolar Path (°C)
5	-7.47 ± 3.82	8.37 ± 2.65
50	-7.08 ± 3.57	7.93 ± 2.58
100	-6.60 ± 3.67	7.39 ± 2.50
350	-4.92 ± 4.14	4.76 ± 2.67

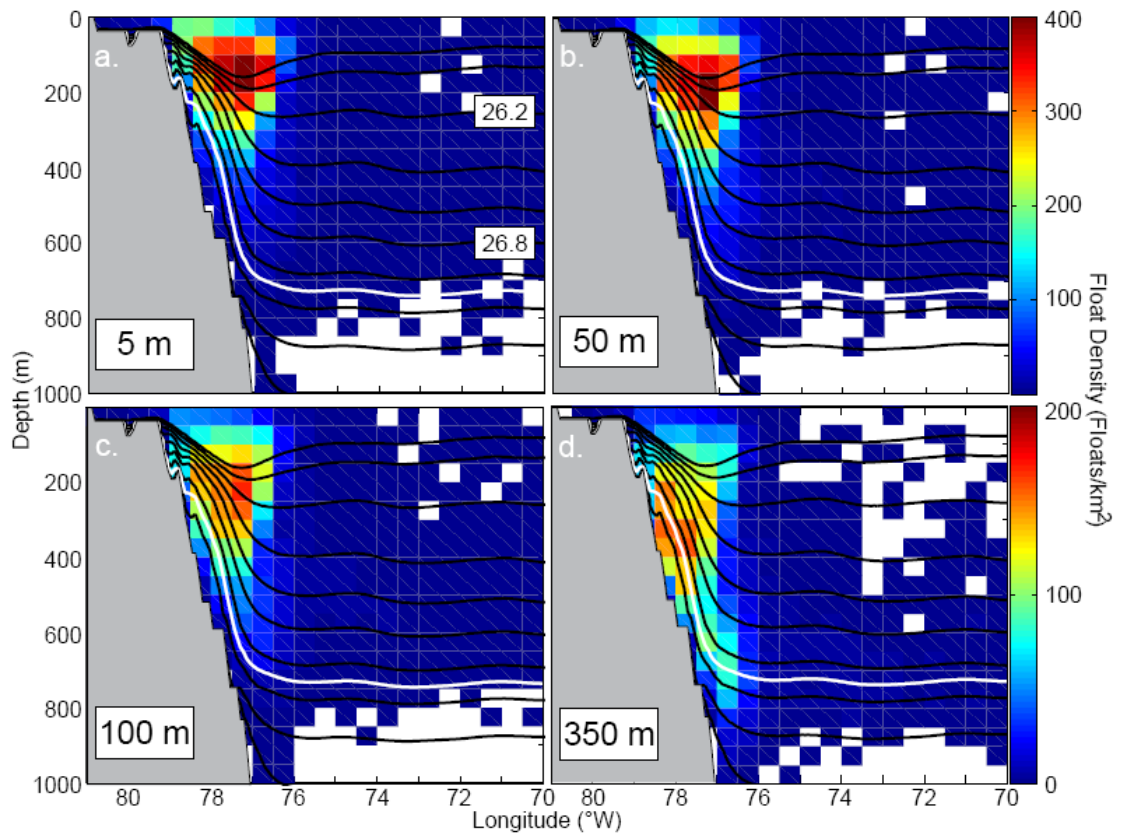


Figure 28: Density contours in the western subtropical gyre superposed over float density plots for those floats arriving at 32°N. Launch locations of the floats when initiated in the ESG are (a) 5 m (b) 50 m (c) 100 m and (d) 350 m. Bathymetry at 32°N is shown in gray. The contour interval is 0.2 kg/m³ for solid black lines. The white line indicates the position of the 27.1 isopycnal.

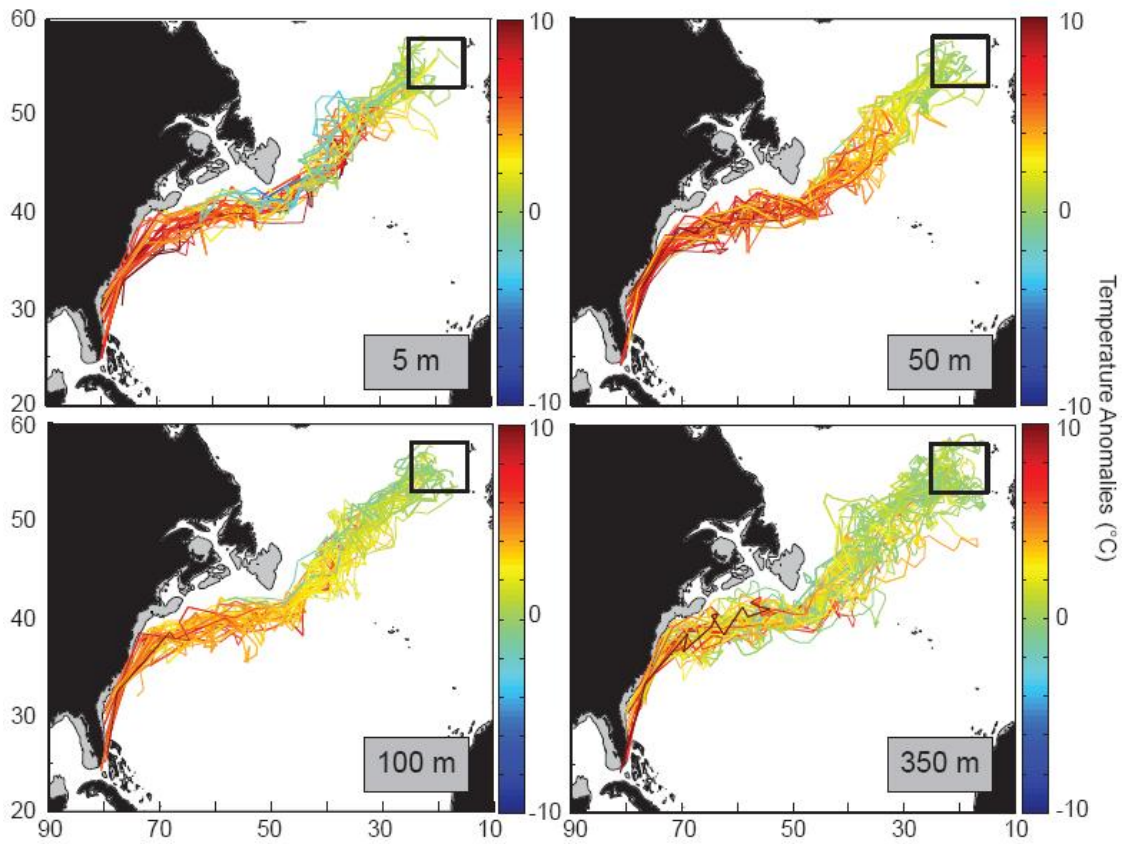


Figure 29: Temperature anomalies of 50 randomly selected floats launched at (a) 5 m (b) 50 m (c) 100 m and (d) 350 m in the ESG as they are run backwards in time to their origin in the western subtropical gyre. Colors indicate the difference in the temperature of the floats at a particular time and their temperature at the time of their launch in the ESG. Bathymetry ≤ 100 m is shown in gray.

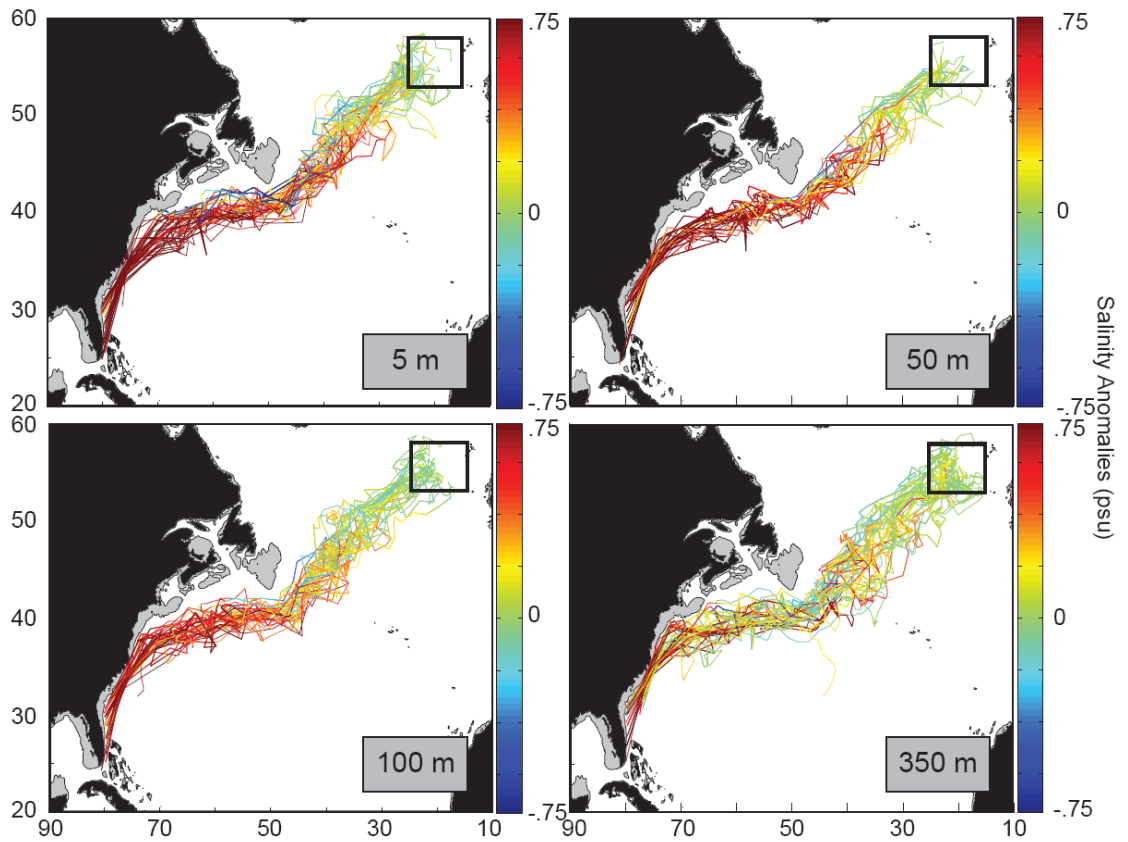


Figure 30: Salinity anomalies of 50 randomly selected floats launched at (a) 5 m (b) 50 m (c) 100 m and (d) 350 m in the ESG as they are run backwards in time to their origin in the western subtropical gyre. Bathymetry ≤ 100 m is shown in gray.

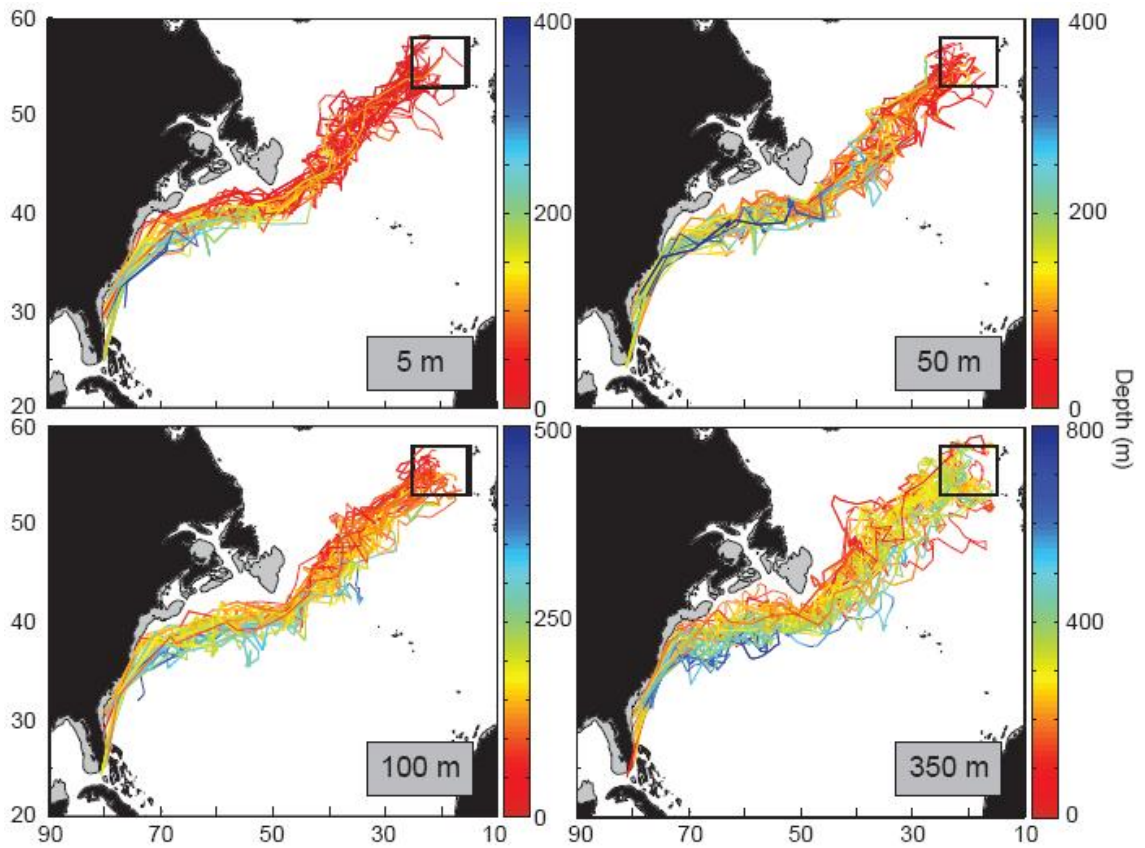


Figure 31: Depths of 50 randomly selected floats launched at (a) 5 m (b) 50 m (c) 100 m and (d) 350 m in the ESG as they are run backwards in time to their origin in the western subtropical gyre. Bathymetry ≤ 100 m is shown in gray.

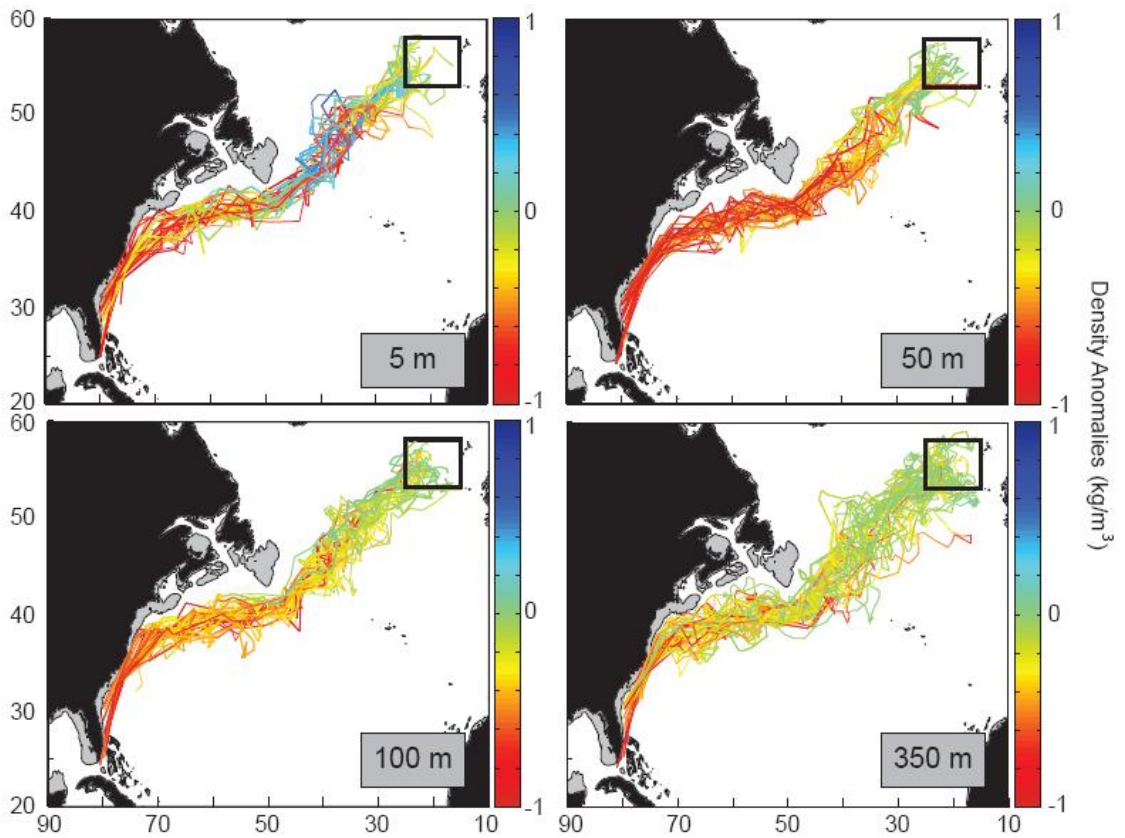


Figure 32: Density anomalies of 50 randomly selected floats launched at (a) 5 m (b) 50 m (c) 100 m and (d) 350 m in the ESG as they are run backwards in time to their origin in the western subtropical gyre. Colors indicate the difference in the density of the floats at a particular time and their density at the time of their launch in the ESG. Bathymetry ≤ 100 m is shown in gray.

4.3.2 Connection to *Burkholder and Lozier (2011)*

The results from this study and those from BL indicate that the transport of waters from the subtropical to the subpolar gyre primarily occurs subsurface. The BL results indicate that the maximum probability of intergyre exchange occurs for floats launched at 700 m in the subtropical gyre (Figure 17). As described in Section 3.4.2, the 700 m floats largely follow isopycnal surfaces as they progress northwards, experiencing only a $\sim 0.1 \text{ kg/m}^3$ densification between the subtropical gyre and 53°N . The target depth of these floats when they cross 53°N is, on average, 350 m. On the other hand, reverse trajectory floats launched at a depth of 350 m from the ESG cross 32°N at an average depth of ~ 380 m, with an average change in density of $\sim 0.7 \text{ kg/m}^3$ between the subtropical and subpolar gyres, a densification more in line with the floats launched at 200 m in the BL study. To explain this apparent difference, we note that in the BL study, floats were seeded throughout the northwestern subtropical gyre, not preferentially in the Gulf Stream. Thus, it is likely that a portion of the floats that reached 53°N within 4 years originated south of the Gulf Stream in the interior of the subtropical gyre. In contrast, the 350 m subpolar reverse launches preferentially track back to the high velocity core of the Gulf Stream/North Atlantic Current.

An investigation of Figure 33, which recreates Figure 17 in density space, indicates that floats in the $\sigma_\theta = 27.1\text{-}27.2$ density range (which lies at ~ 700 m in the interior of the subtropical gyre and shoals within the Gulf Stream, Figure 28) were the most successful

at exiting the subtropical gyre and reaching high latitudes when launched from the BL grid. The presence of floats in the $\sigma_{\theta} = 27.1-27.2$ density range is also apparent in the reverse launches from the ESG at 350 m (Figure 28d), although, not surprisingly, at 32°N these floats lie at depths shallower than 700 m. Since the first entry of the floats into the subtropical gyre is marked in Figure 28d, the shallower depths of the 27.1-27.2 floats indicate merely that the floats launched offshore of the Gulf Stream in the BL study shoaled significantly as they were entrained into the Gulf Stream on their way to the subpolar gyre. However, though the presence of the 27.1-27.2 density class is obvious in Figure 28d, evidence of a number of lighter floats is also apparent: the mean density of floats at 32°N is 26.7 kg/m^3 . In order to understand this lighter mean density, we examine a second float population density map (Figure 34) for the 350 m floats compiled at 63°W (the center longitude of the BL subtropical launch box). The floats at 63°W also indicate lower mean densities than those involved in the intergyre exchange process in the BL study ($\sigma_{\theta} = 27.1 \text{ kg/m}^3$). Clearly, waters less dense than those highlighted in the BL study impact the ESG.

Putting the depth and density destinations of the forward and reverse launches together, we conclude that floats launched at 700m have a greater chance of reaching the subpolar gyre, but that the waters that constitute the ESG region have their origin shallower than 700m (and lighter than 27.1) in the Gulf Stream. Although these shallower and lighter waters, on average, have less of a chance to reach the subpolar gyre, their transport is larger than that at 700m and, as indicated by the reverse launches, they play a larger role

in setting the destination properties than might have been suspected from the forward launch scheme only.

4.4 Summary

The zonal asymmetry in the SST fields of the subpolar gyre has been recognized for years as an important source of heat to the atmosphere, raising temperatures in Western Europe to $>10^{\circ}\text{C}$ above the zonal average temperatures at high latitudes. Although the importance of this SST asymmetry has long been understood, the sources of heat to the climactically important ESG have never been fully established. With this work, we use launches of synthetic floats in a high resolution model of ocean circulation to identify and characterize the key pathways that supply the ESG. Though two pathways were identified, the pathway that was determined to be the dominant source of heat to the ESG was the subtropical pathway, which transports floats from mid-depths in the subtropics directly to high latitudes.

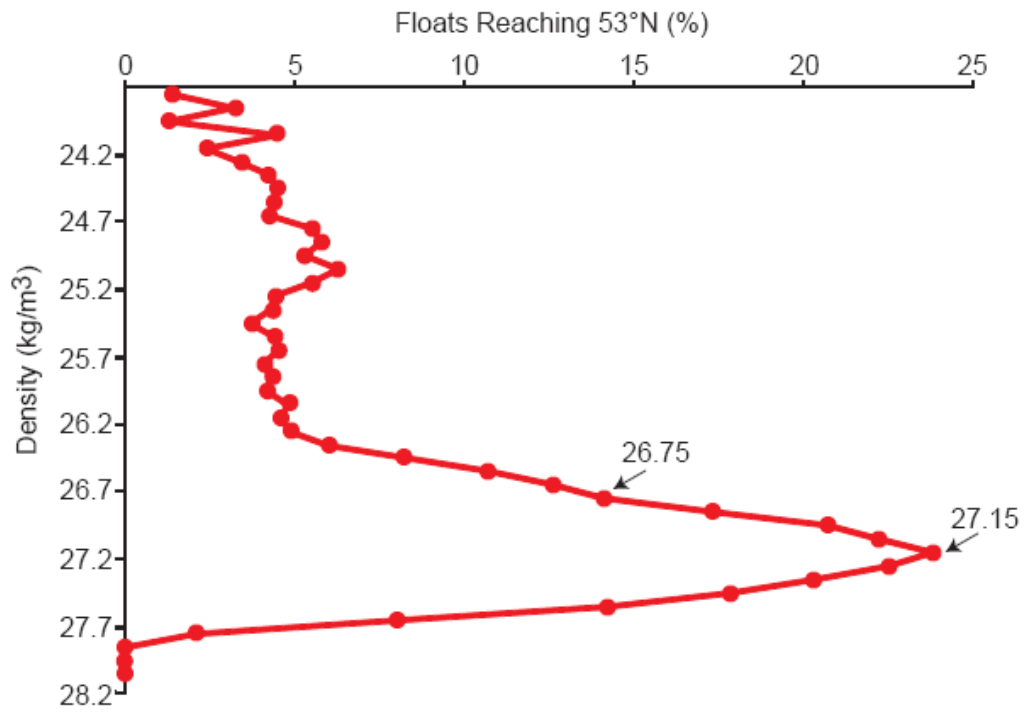


Figure 33: Re-creation of Figure 17 in density space, showing the fraction of BL floats launched below the Ekman layer in the subtropical gyre that reached 53°N within 4 years. Floats launched between 27.1 and 27.2 in the subtropical gyre were the most successful in reaching 53°N.

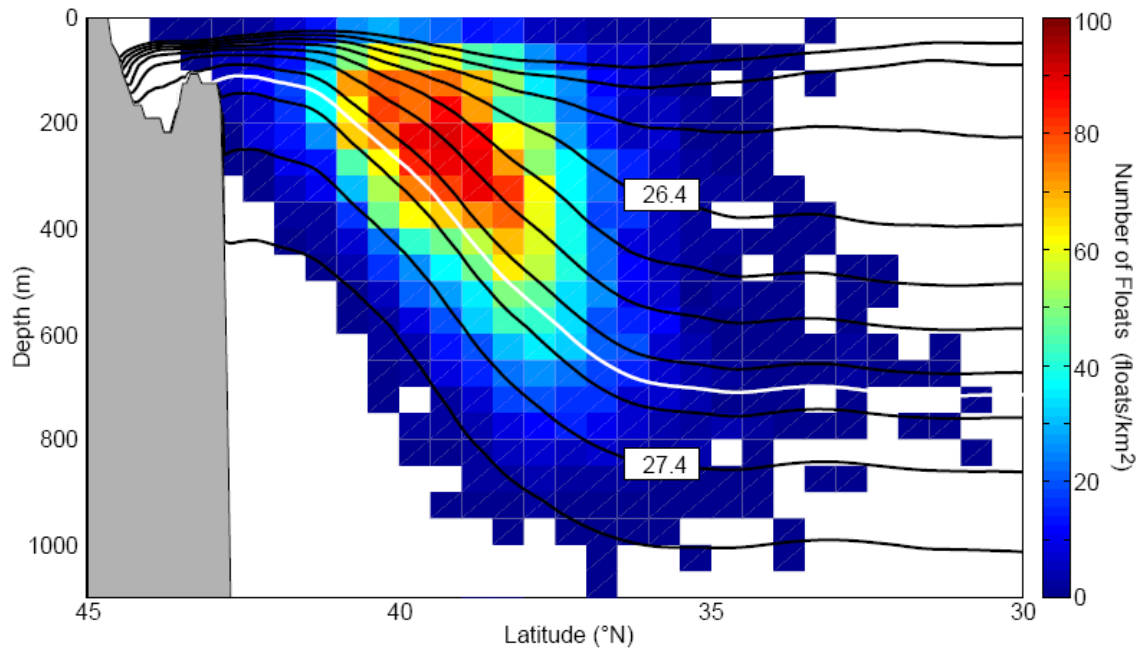


Figure 34: Contours of potential density at 63°W superposed over population density of floats crossing that line of longitude when launched at 350 m in the ESG box. Bathymetry at 63°W is shown in gray. The contour interval is 0.2 kg/m³ for solid black lines. The white line indicates the climatological position of the 27.1 isopycnal.

References

- Arhan, M., de Verdière, A.C., and L. Mémerly, 1994. The Eastern Boundary of the Subtropical North Atlantic. *J. Phys. Oceanogr.*, **24**, 1295-1316.
- Bersch, M., Meincke, J., and A. Sy, 1999. Interannual thermohaline changes in the northern North Atlantic 1991-1996. *Deep Sea Res. Part 2 Top. Stud. Oceanogr.*, **46**, 55-75.
- Bersch, M., Yashayaev, I. and K.P. Koltermann, 2007. Recent changes in the thermohaline circulation in the subpolar North Atlantic. *Ocean Dynamics*, **57**, 223-235.
- Biastoch, A., C.W. Böning, J. Getzlaff, J. Molines and G. Madec (2008), Causes of interannual-decadal variability in the meridional overturning circulation of the midlatitude North Atlantic Ocean, *Journal of Climate*, *21*, 6599-6615. doi: 10.1175/2008JCLI2404.1
- Böning, C.W., M. Scheinert, J. Dengg, A. Biastoch and A. Funk (2006), Decadal variability of subpolar gyre transport and its reverberation in the North Atlantic overturning, *Geophysical Research Letters*, *33*, L21S01. doi: 10.1029/2006GL026906
- Bower, A. S. and M. S. Lozier (1994), A closer look at particle transport in the Gulf Stream, *Journal of Physical Oceanography*, *24*(6), 1399-1418.
- Bower, A.S., B. Le Cann, T. Rossby, W. Zenk, J. Gould, K. Speer, P.L. Richardson, M.D. Prater and H.M. Zhang, 2002. Directly measured mid-depth circulation in the northeastern North Atlantic Ocean. *Nature*, **419**, 603-607.
- Boyer, T.P., J.I. Antonov, H.E. Garcia, D.R. Johnson, R.A. Locarnini, A.V. Mishonov, M.T. Pitcher, O.K. Baranova, I.V. Smolyar, 2006. World Ocean Database 2005. S. Levitus, Ed., NOAA Atlas NESDIS 60, U.S. Government Printing Office, Washington, D.C., 190 pp., DVDs.
- Brauch, J.P., and R. Gerdes, 2005. Response of the northern North Atlantic and Arctic oceans to a sudden change of the North Atlantic Oscillation. *J. Geophys. Res.*, **110**, C11018.
- Brambilla, E., and L. D. Talley (2006), Surface drifter exchange between the North Atlantic subtropical and subpolar gyres, *J. Geophys. Res.*, *111*(C7), C07026. doi: 10.1029/2005jc003146

Cunningham, S. A., T. Kanzow, D. Rayner, M. O. Baringer, W. E. Johns, J. Marotzke, H. R. Longworth, E. M. Grant, J. J. M. Hirschi, L. M. Beal, C. S. Meinen and H. L. Bryden (2007), Temporal Variability in the Atlantic Meridional Overturning Circulation at 26.5°N, *Science*, 317, 935. doi: 10.1126/science.1141304

Curry, R.G., 1996. HydroBase: A database of hydrographic station and tools for climatologic analysis. *WHOI Technical Report*, 96-01, 55 pp.

Curry, R.G. and M.S. McCartney, 2001. Ocean gyre circulation changes associated with the North Atlantic Oscillation. *J. Phys. Oceanogr.*, **31**, 3374-3400.

Deshayes, J. and C. Frankignoul, 2008. Simulated variability of the circulation in the North Atlantic from 1953-2003. *J. Clim.*, **21**, 4919-4933.

Ducet, N., P.-Y. Le Traon, and G. Reverdin, How accurately can we map the mesoscale ocean surface variability from the combination of T/P and ERS-1/2 altimetric data?, *Int. WOCE Newsl.*, 37, 40-43, 1999.

Eden, C. and J. Willebrand, 2001. Mechanism of Interannual to Decadal Variability of the North Atlantic Circulation. *J. Clim.*, **14**, 2266- 2280.

Ellet, D.J., Edwards, A. and Bowers, R., 1986. The hydrography of the Rockall Channel, an overview. *Proc. R. Soc. Edinb. Biol.*, 88B, 61-81.

Flatau, M. K., L. Talley and P. P. Niiler (2003), The North Atlantic Oscillation, Surface Current Velocities, and SST Changes in the Subpolar North Atlantic, *Journal of Climate*, 16(14), 2355-2369. doi:10.1175/2787.1

Fratantoni, D. M. (2001), North Atlantic surface circulation during the 1990's observed with satellite-tracked drifters, *J. Geophys. Res.*, 106(C10), 22067-22093. doi: 10.1029/2000jc000730

Fuglister, F.C., and A.D. Voorhis (1965), A new method for tracking the Gulf Stream, *Limnol. Oceanogr.* Supplement to 10:R115-R124.

Furey, H.H., A.S. Bower and P.L. Richardson, 2001. Warm Water Pathways in the Northeastern North Atlantic ACCE RAFOS Float Data Report November 1996-November 1999.

Gary, S. F., M. S. Lozier, C. W. Böning and A. Biastoch (2011), Deciphering the pathways for the deep limb of the Meridional Overturning Circulation, *Deep Sea Research*, in press.

- Ganachaud, A. (2003), Large-scale mass transports, water mass formation, and diffusivities estimated from World Ocean Circulation Experiment (WOCE) hydrographic data, *Journal of Geophysical Research*, 108(C7), 3213. doi: 10.1029/2002JC001565
- Gordon, A. L. (1986), Inter-ocean exchange of thermocline water, *Journal of Geophysical Research-Oceans*, 91(C4), 5037-5046.
- Hall, M. M. and H. L. Bryden (1982), Direct estimates and mechanisms of ocean heat transport, *Deep-Sea Research*, 29(3A), 339-359.
- Hakkinen, S., and P. B. Rhines (2009), Shifting surface currents in the northern North Atlantic Ocean, *J. Geophys. Res.*, 114(C4), C04005. doi: 10.1029/2008jc004883
- Hátún, H., Sandø, A.B., Drange, H., Hansen, B., and H. Valdimarsson, 2005. Influence of the Atlantic subpolar gyre on the thermohaline circulation. *Science*, **309**, 1841-1844.
- Holliday, N.P., R.T. Pollard, J.F. Read and H. Leach, 2000. Water mass properties and fluxes in the Rockall Trough: 1975 to 1998, *Deep Sea Res. Part 1 Oceanogr. Res. Pap.*, **47**, 1303-1332.
- Holliday, N.P., 2003. Air-sea interaction and circulation changes in the northeast Atlantic. *J. Geophys. Res.*, **108**, 3259. doi: 10.1029/2002JC001344
- Hogg, N. G., R. S. Pickart, R. M. Hendry and W. J. Smethie, Jr. (1986), The northern recirculation gyre of the gulf Stream, *Deep Sea Research Part A. Oceanographic Research Papers*, 33(9), 1139-1165.
- Hurrell, J.W., 1995. Decadal trends in the North Atlantic Oscillation: Regional temperatures and precipitation. *Science*, **269**, 676-679.
- Iorga, M.C. and M.S. Lozier, 1999a. Signatures of the Mediterranean outflow from a North Atlantic climatology: Salinity and density fields. *J. Geophys. Res.*, **104**, 25985-26009.
- Iorga, M.C. and M.S. Lozier, 1999b. Signatures of the Mediterranean outflow from a North Atlantic climatology: Diagnostic velocity fields. *J. Geophys. Res.*, **104**, 26011-26029.
- Lozier, M. S. (2010), Deconstructing the Conveyor Belt, *Science*, 328(5985), 1507-1511. doi: 10.1126/science.1189250

Lozier, M. S., and S. C. Riser (1990), Potential Vorticity Sources and Sinks in a Quasi-geostrophic Ocean: beyond Western Boundary Currents, *Journal of Physical Oceanography*, 20(10), 1608-1627. doi: 10.1175/1520-0485(1990)020<1608:PVSASI>2.0.CO;2

Lozier, M.S. and N.M. Stewart, 2008. On the temporally varying northward penetration of Mediterranean Overflow Water and eastward penetration of Labrador Sea Water. *J. Phys. Oceanogr.*, **38**, 2097-2103.

Lozier, M.S., W.B. Owens and R.G. Curry, (1995). The Climatology of the North Atlantic. *Prog. Oceanogr.*, **36**, 1-44.

McCartney, M. and L. Talley (1982), The Subpolar Mode Water of the North Atlantic Ocean, *Journal of Physical Oceanography*, 12(11), 1169-1188.

McCartney, M.S. and C. Mauritzen, 2001. On the origin of the warm inflow to the Nordic Seas. *Prog. Oceanogr.*, **51**, 125-214.

Niiler, P. P., A. S. Sybrandy, K. Bi, P. M. Poulain and D. Bitterman (1995), Measurements of the water-following capability of holey-sock and TRISTAR drifters, *Deep Sea Research I*, 42(11-12), 1951-1964. doi: 10.1016/0967-0637(95)00076-3

Pazan, S. E., and P. P. Niiler (2001), Recovery of Near-Surface Velocity from Undrogued Drifters, *Journal of Atmospheric and Oceanic Technology*, 18(3), 476-489. doi: 10.1175/1520-0426(2001)018<0476:RONSVF>2.0.CO;2

Price, J. F., and M. A. Sundermeyer (1999), Stratified Ekman layers, *J. Geophys. Res.*, 104(C9), 20467-20494. doi: 10.1029/1999jc900164

Qiu, B., and R. X. Huang (1995), Ventilation of the North Atlantic and North Pacific: Subduction Versus Obduction, *Journal of Physical Oceanography*, 25(10), 2374-2390. doi: 10.1175/1520-0485(1995)025<2374:VOTNAA>2.0.CO;2

Reid, J., 1979. On the contribution of the Mediterranean Sea outflow to the Norwegian-Greenland Sea. *Deep Sea Res. A*, **26a**, 1199-1223.

Rhines, P. B., and R. Schopp (1991), The Wind-driven Circulation: Quasi-geostrophic Simulations and Theory for Nonsymmetric Winds, *Journal of Physical Oceanography*, 21(9), 1438-1469. doi: 10.1175/1520-0485(1991)021<1438:TWDCQG>2.0.CO;2

Roemmich, D. and C. Wunsch (1985), Two transatlantic sections: meridional circulation and heat flux in the subtropical North Atlantic Ocean, *Deep Sea Research*, 32(6), 619-664.

Sarafanov, A., Falina, A., Sokov, A. and A. Demidov, 2008. Intense warming and salinification of intermediate waters of southern origin in the eastern subpolar North Atlantic in the 1990s to mid-2000s. *J. Geophys. Res.*, **113**, C12022.4.

Schmitz, W.J. Jr. and M. S. McCartney (1993), On the North Atlantic Circulation, *Review of Geophysics*, 31(1), 29-49.

Schott, F. and H.M. Stommel (1978), Beta spirals and absolute velocities in different oceans, *Deep Sea Research*, 25(11), 961-1010. doi: 10.1016/0146-6291(78)90583-0

Spall, M. (1992), Cooling Spirals and Recirculation in the Subtropical Gyre, *Journal of Physical Oceanography*, 22(5), 564-571. doi:10.1175/1520-0485(1992)022<0564:CSARIT>2.0.CO;2

Stommel, H. (1958), The Abyssal Circulation, *Deep Sea Research*, 5, 80.

U.S. Department of Commerce, National Oceanic and Atmospheric Administration, National Geophysical Data Center, 2006. *2-minute Gridded Global Relief Data (ETOPO2v2)* <http://www.ngdc.noaa.gov/mgg/fliers/06mgg01.html>

Willis, J. K. (2010), Can in-situ floats and satellite altimeters detect long-term changes in Atlantic Ocean overturning?, *Geophysical Research Letters*, 37, L06602. doi: 10.1029/2010GL042372

Biography

Kristin Burkholder was born in Springfield, Massachusetts on May 2, 1984. She grew up in Marblehead, MA and graduated from Marblehead High School in 2002. She then attended Bucknell University, graduating with a Bachelor of Science degree in chemistry in 2006. While at Bucknell, she spent a summer participating in the Sea Education Association's summer program which allowed her a taste of oceanographic research during a summer spent on Cape Cod and sailing between Hawaii and San Francisco. That experience, coupled with the love of the ocean that she had fostered since her childhood in Massachusetts, led her to pursue a graduate degree in physical oceanography at Duke University, which she began in the fall of 2006. Since then, she has completed two projects for publication:

- (1) Burkholder, K. C., and M. S. Lozier (2011), Subtropical to subpolar pathways in the North Atlantic: Deductions from Lagrangian trajectories, *J. Geophys. Res.*, 116, C07017, doi:10.1029/2010JC006697.
- (2) Burkholder, K. C. and M. S. Lozier (2011), Lagrangian Pathways in the Eastern North Atlantic and their Impact on High Latitude Salinities. *Deep Sea Research*, accepted.

Kristin currently lives in Roanoke, Virginia with her husband Andrew and her black lab, Riley.